

# Design and investigation of PV string/central architecture for bayesian fusion technique using grey wolf optimization and flower pollination optimized algorithm

Hemalatha S<sup>a,\*</sup>, Johny Renoald A<sup>b</sup>, Banu G<sup>c</sup>, Indirajith K<sup>d</sup>

<sup>a</sup> Department of EEE, St. Joseph's Institute of Technology, Chennai, Tamilnadu, India

<sup>b</sup> Department of EEE, Erode Sengunthar Engineering College, Perundurai, Tamilnadu, India

<sup>c</sup> Department of EEE, VSB College of Engineering Technical Campus, Coimbatore, Tamilnadu, India

<sup>d</sup> Department of EEE, Erode Sengunthar Engineering College, Perundurai, Tamilnadu, India

## ARTICLE INFO

### Keywords:

Grey Wolf Optimization algorithm  
Flower Pollination Algorithm  
Partially Shading Condition  
Bayesian Fusion Technique Maximum Power Point  
Photovoltaic array

## ABSTRACT

One of the most essential factors in the current study is effectively harvesting the Maximum Power Extraction (MPE) from the Photovoltaic (PV) panel. The primary difficulties in extracting solar power is occurrence of partial shading which causes the panel to significantly increases power loss. These will mainly occur due to when partially shaded solar PV array kept under certain critical conditions for obtaining maximum output power. Many researcher have suggested by connecting bypass diodes in anti-parallel to the PV modules hotspots in the modules can be avoided. Out of all techniques, the proposed Bayesian Fusion Technique (BFT) is a hybrid optimization algorithm that combines the Grey Wolf Optimization (GWO) and Flower Pollination Algorithm (FPA) techniques to optimize the performance of solar panels in photovoltaic (PV) systems. The combination of GWO and FPA forms an ideal combination that is beneficial for optimizing the performance of PV systems is determined in this work. In this study real 6\*6 PV array string and irregular PV array configuration such as central and parallel-series PV string combination of various partial shading pattern is compared and found to be effective for reducing the hotspots problems. The performance of these configuration under different shading patterns have been compared and analyzed with the different parameters like output power, conversion efficiency and tracking efficiency. This article state about the influence of partial darkening and the crucial point that reduce the sensitivity to shading heaviness. For better understanding for reader the MATLAB/Simulink software is used to validate the simulation result with real time data. Overall, this article states the BFT is an efficient and reliable approach to improve the efficiency of PV systems, by combining two optimization techniques like GWO and FPA hybrid algorithm. This article gives clear insight to the researchers for choosing BFT-GWO algorithm in order to decrease the cost and wastage of energy for achieving better solar panel performance.

## 1. Introduction

Nowadays, electricity requirement for domestic and industry keep on increasing day by day. Conventional energy sources have the following disadvantages like exhaustible, overpriced, and also pass off smoke and

slag. In [1-6], non-conventional energy resources including fuel cells, wind, solar, and biogas are optimal for replacing conventional energy sources. Compared to other renewable power, the solar energy has more advantages. It produces no pollution, it needs minimal maintenance, no cost for fuel. It is easily available in the environment. Among all noteworthy facts solar panel affect by external factors such as Lighting,

*Abbreviations:* MPE, Maximum Power Extraction; PV, Photovoltaic; BFT, Bayesian Fusion Technique; GWO, Grey Wolf Optimization; FPA, Flower Pollination Algorithm; MP, Maximum power; FL, Fuzzy logic; ANN, artificial neural networks; SI, Swarm Intelligence; GBAS, Grouped Beetle Antennae Search; GA, Genetic Algorithm; MPPT, Maximum Power Point Tracking; PSC, Partial shading conditions; BFT-MPP, Bayesian Fusion Technique Proposal Maximum Power; V-I, Voltage to current; TCTPV, Total-Cross Tied PV; P-V, Power-Voltage; S-PV, Solar photovoltaic; PMW, Pulse with modulation; D, Diode; A, Amps; V-P, Voltage to power; IGBT, Insulated-Gate Bipolar Transistor; CTP, Conditional probability table; MPP, Maximum Power Point;  $G_{MPP}$ , Global maximum power point; BFOT, Bayesian Fusion Optimization Technique;  $P_{loss_{IGBT}}$ , Power losses in Insulated-Gate Bipolar Transistor;  $P_{loss_{inductor}}$ , Power losses in inductor.

\* Corresponding author.

E-mail address: [hodeeelabaffairs@stjosephstechnology.ac.in](mailto:hodeeelabaffairs@stjosephstechnology.ac.in) (H. S).

<https://doi.org/10.1016/j.enconman.2023.117078>

Received 7 January 2023; Received in revised form 15 April 2023; Accepted 17 April 2023

Available online 26 April 2023

0196-8904/© 2023 Elsevier Ltd. All rights reserved.

Nomenclature			
<i>List of Symbol</i>		pF	Power factor
<b>Symbols Meaning</b>		$V_{GE}$	Gate emitter voltage
$W/m^2$	Radian meter square	$t_{fall}$	Fall time
DC-DC	Direct current to direct current	$R_{fall}$	Raise time
DC	Direct current	W	Watts
$I_{MPP}$	Maximum power point current	KHz	kilohertz
T	Time in seconds	$W/m^2$	Watt meter square
I	Current in amps	$V_{oc}$	Open circuit voltage
V	Voltage in volts	$V_{sc}$	Short circuit voltage
$\eta$	Efficiency	$\alpha$	Alpha
$I_{PV}$	Photovoltaic current	$\beta$	Beta
$V_{PV}$	Photovoltaic voltage	$\delta$	Delta
$V_o$	Output Voltage	D	Duty cycle
$I_o$	Output current	$P_{max}$	Maximum power
L	Inductor	$P_{in}$	Input power
D	Diode	Gbest	Global best
$C_{in}$	Input capacitor	$T_S$	Sampling period
A	Ammeter	$\Omega$	Ohm
V	Voltmeter	$^{\circ}C$	Celsius
$V_{in}$	Input voltage	t	Time
$V_{out}$	Output voltage	$I_{sc}$	Short circuit current
$P_{loss}$	Power loss	$I_{oc}$	Open circuit current
$I_c$	Collector current	$I_{mp}$	Current at maximum power
$I_{RMS}$	Root mean square current	$P_{PV}$	Photovoltaic power
$V_{CE}$	Collector to emitter voltage	$P_o$	Output power
$F_{SW}$	Switching frequency	ns	Nano seconds
$R_{on}$	Resistance ON condition	nv	Nano voltage
$I_C^2$	Collector current	$R_{DC}$	Resistance in direct current
$Q_g$	Total is total gate charge	$\Gamma(\lambda)$	Gamma function
$C_{oes}$	Output capacitance co-efficient	$X_K$	Iteration candidate position(k)
$I_{RMSDIODE}$	Root mean square current diode	$X_{\alpha_k}, X_{\beta_k}, X_{\delta_k}$	Wolves position in iteration (k)
$P_{LOSS\ diode}$	Power loss diode	i	Current best solution
$V_F$	Forward voltage	G	Global best solution
		L	Strength of the pollination
		N	Group of flowers

temperature, and dust are inevitable. Therefore, the entire research world is trying to figure this out, traditional system more concern about longevity. Impairment of this device are mainly affect by panel design, which determine how much electricity a PV panel can produce. When there are shading circumstances, among the section of the different panels affected by trees, castles, dust and high – rise buildings to complicate produce good efficiency. As a result, the panel generates the minimum output power as well as more peak power [7]. Hence under partial shading condition the extraction of maximum power (MP) is complicated from the solar panel.

To extract maximum power form Solar-PV (S-PV) under uniform and PSC (Partial shading conditions) and an optimization technique is necessary. Various optimization techniques have been created and tested throughout the years, based on convergence time and equipment implementation. Perturb and Observe (P&O) and Incremental Conductance are the most often used traditional approaches [7]. However, many techniques are user-friendly of straightforward design. When there is a panel under PSC, it can be unable to locate the exact global peak output and local peak output. The performance of the pumping system is improved by combining Fuzzy Logic (FL) with artificial neural networks (ANN) [8]. According to the literature, this may not be the circumstance for many researchers used traditional MPP techniques such Artificial Neural Networks (ANN) and Fuzzy Logic Control (FLC) to solve extraction problems in PV panels, which is required fuzzification, rule basis, and defuzzification processes. Following that, more number of Swarm Intelligence (SI) approaches are described and established. PSO was utilized as an optimization strategy in various solar irradiance

conditions [9], but the resulting outcome as longer convergence rate, computational speed/time were observed [10] and also poor local search capabilities are observed due to the lack of crossover and mutation process. Renewable energy is being encouraged all around the world due to the pollution generated by fossil fuels. Solar energy is one of the most important of these energy sources. Since, it is cheap and does not pollute the environment. The major advantage of solar photovoltaic (PV) technology, which is immediately turns sunlight into the power without any disturbance. As per the result of input source, it is strongly recommended and compared to other renewable energy sources.

The proposed BFT combines the advantages of GWO and FPA and uses Bayesian theories to optimize their combination. The BFT approach creates a new search space and then adjusts the parameters of GWO and FPA to obtain the best optimization results for any given problem. When a specific critical point is reached, hotspot arises. Among all notable fact, this phenomenon occurs due to increases in temperature at shaded part of PV module during the reverse bias condition. Bayesian Fusion is a technique used to combine probabilistic models of different types of sensor data to provide a more comprehensive view of a particular environment. This technique is particularly useful in the field of solar panel design, as it allows for the combination of surveys of potential locations for panels with satellite imaging to better assess the most effective and efficient locations to install solar panels.

In the simulated annealing and the (FPA) Flower Pollination Algorithm are combined to enhance the PV tracking optimization performance for improving the convergence rate. But, the FPA and Grey Wolf Optimization (GWO) methods are used only for core architecture [11].

**Table 1a**  
Different partial shading patterns.

Solar PV array shading position	PV array	Irradiances
Centre shading	PV1,PV6 and PV12	200 W/m <sup>2</sup>
	PV1,PV7 and PV13	300 W/m <sup>2</sup>
	PV1,PV8 and PV14	400 W/m <sup>2</sup>
	PV1,PV9 and PV15	500 W/m <sup>2</sup>
Corner shading	PV1,PV10 and PV16	300 W/m <sup>2</sup>
	PV1,PV11 and PV17	400 W/m <sup>2</sup>
	PV1,PV12 and PV18	500 W/m <sup>2</sup>
	PV1,PV13 and PV19	600 W/m <sup>2</sup>
	PV1,PV14and PV20	400 W/m <sup>2</sup>
	PV1,PV15 and PV21	500 W/m <sup>2</sup>
Right side end shading	PV1,PV16and PV22	600 W/m <sup>2</sup>
	PV1,PV17 and PV23	700 W/m <sup>2</sup>
	PV1,PV18and PV22	400 W/m <sup>2</sup>
	PV1,PV19 and PV23	500 W/m <sup>2</sup>
Frame shading	PV1,PV20 and PV24	600 W/m <sup>2</sup>
	PV1,PV21 and PV25	700 W/m <sup>2</sup>
	PV1,PV22and PV26	400 W/m <sup>2</sup>
	PV1,PV23 and PV27	500 W/m <sup>2</sup>
	PV1,PV24 and PV28	600 W/m <sup>2</sup>
Diagonal shading	PV1,PV25 and PV29	700 W/m <sup>2</sup>
	PV1,PV26 and PV30	800 W/m <sup>2</sup>
	PV1,PV27and PV31	900 W/m <sup>2</sup>
	PV1,PV28 and PV32	1000 W/m <sup>2</sup>
	PV1,PV29 and PV33	1100 W/m <sup>2</sup>
	PV1,PV30 and PV33	1200 W/m <sup>2</sup>
Bottom side shading	PV1,PV31 and PV34	1300 W/m <sup>2</sup>
	PV1,PV32 and PV35	1400 W/m <sup>2</sup>
	PV1,PV33 and PV36	1500 W/m <sup>2</sup>
	Random shading conditions.	

Grouped Beetle Antennae Search (GBAS), existing method was employed [12,13] to determine the Solar-PV array structures in three separate models. Genetic Algorithm (GA)-FPA was used in to estimate the convergence accuracy and speed optimization process. According to one of the most crucial features for photovoltaic (PV) systems is maximum power harvest, and in order to achieve this correct modeling and steady state operation of solar cells were essential to be discussed. In this research, characteristics such as convergence time, accuracy, optimal duty value and PV panel tracking efficiency were obtained and compared with GWO and FPA optimized algorithms for both central and PV string architectures. When compared to other reconfiguration methods, this proposed method needs to operate only with fewer switching networks. In this configuration each module integrates with its own MPPT (Maximum Power Point Tracking) controller and provides

greater power compared with PV string and central architecture. In this research work we have performed new approach for modeling and simulations of PV array under various PSCs condition. Based on the performance metrics, for all PV array configurations are examined and compared in terms of numerous parameters. The contribution of my research work is under PSC and the shading pattern is provided 6\*6 PV array subjected to the different shading positions, which is center shading, corner, right side end shading, bottom side, diagonal, frame, and random shading condition. The V-I characteristics of different solar irradiation level outcome as shown in Fig.1 (a & b). Table.1(a) depicted that different operating partial shading conditions for proposed work.

By combining different pieces of data, Bayesian Fusion can provide a more complete picture of the environment to help inform the decisions involved in determining the optimal locations for solar panels. The integration of two or more MPPT tracking methods based on feature vector building is improved by this conception. Bayesian Fusion Technique Proposal Maximum Power Point (BFT-MPP) is a mathematical fusion structure that is built on the notion of Bayesian decision theory presented. Bayesian Fusion is a technique used to combine probabilistic models of different types of sensor data to provide a more comprehensive view of a particular environment. This technique is particularly useful in the field of solar panel design, as it allows for the combination of surveys of potential locations for panels with better assess the most effective and efficient locations to install solar panels. By combining different pieces of data, Bayesian Fusion can provide a more complete picture of the environment to help inform the decisions involved in determining the optimal locations for solar panels.

The integration of two or more MPPT tracking methods based on feature vector building is improved by this conception. This suggested technique can readily accommodate uncertainties in irradiance and temperature due to its probabilistic approach. In this regard, bio-inspired FPA/GWO approaches aided by INC (Incremental Conductance) might be a promising alternative for improving the efficiency and reliability of BFT-MPP algorithms. Unfortunately, the potential of hybrid approaches is not fully explored in the literature, and switching between the bio-inspired FPA method and the GWO method is done in a relatively shallow manner. As a result, a novel FPA/GWO approach supported by BFT-MPP is suggested in this article. This study incorporates and validates a novel switching method to achieve efficient usage of both the FPA/GWO algorithms. More significantly, the switch doesn't happen until the first FPA exploration of the global power areas. Further, to make an accurate comparison, the FPA-GWO findings are

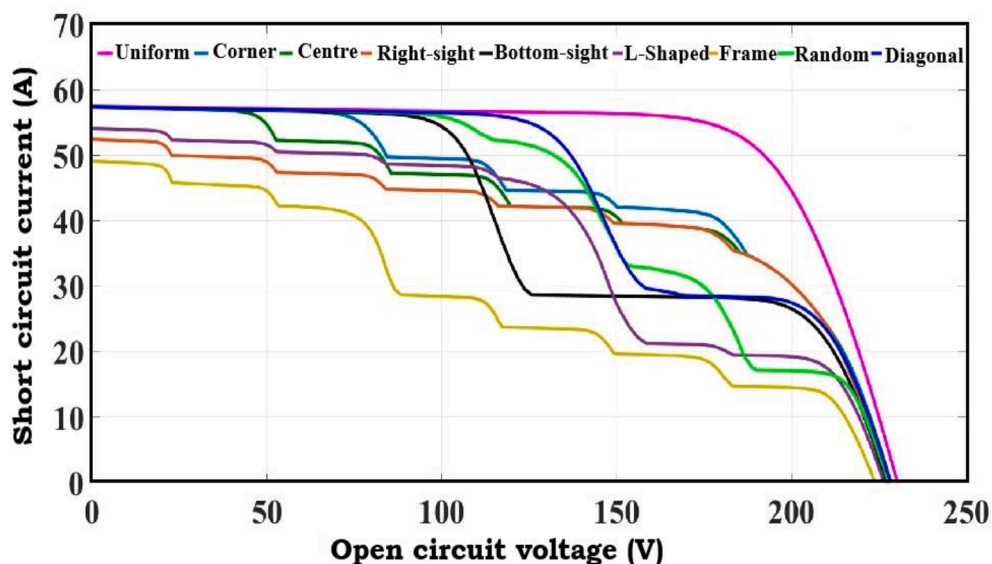


Fig. 1a. 6\*6 PV array configuration V-I characteristics curve.

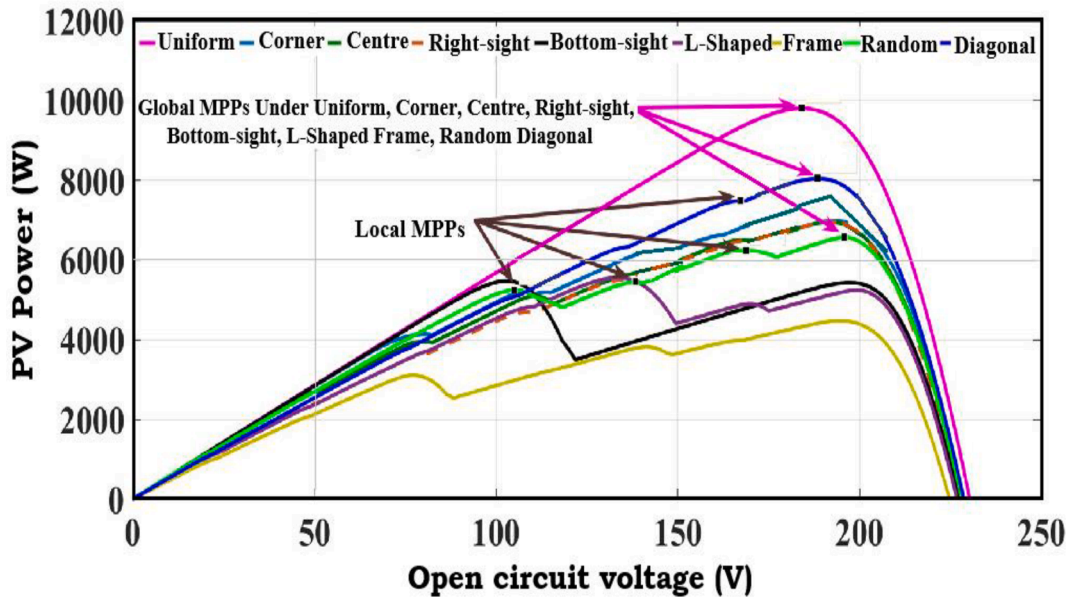


Fig. 1b. 6\*6 PV array configuration P-V characteristics curve.

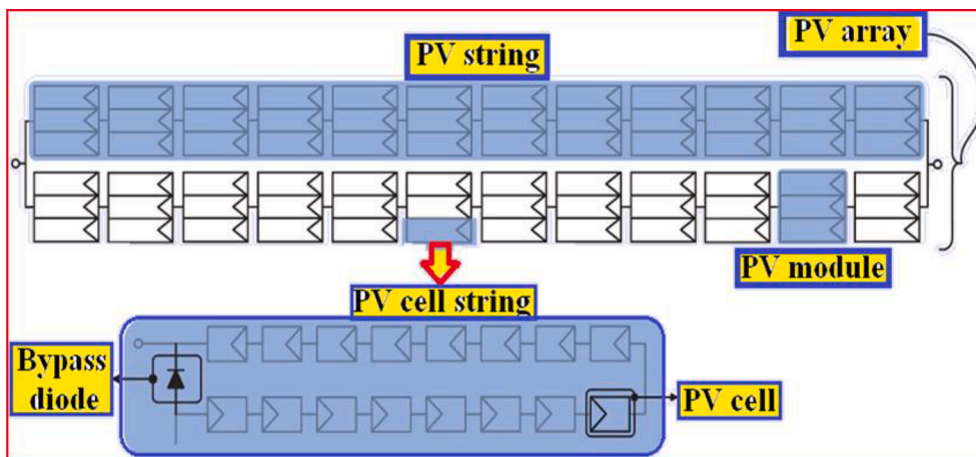


Fig. 2a. Architecture for PV string and PV array.

contrasted with those of recently validated alternative optimization and traditional *meta*-heuristics techniques. The proposed system is local BFT-MPP and global shade dispersion index is calculated and compared with FPA and GWO algorithm techniques. The skeleton of this paper divided into following section. The solar energy conversion system’s output power is enhanced by using effective shade dispersion. The skeleton of the paper is divided into the following section. The real time data were obtained are validated using MATLAB/Simulink (R2019a) tool is used to model the optimization approaches. Section.2 of this study outlines the literature study. Section.3 proposed architecture of solar PV panels BFT-MPP using different algorithm that is validated the optimization strategies with objective derivatives. Section.4 described about the simulation and hardware implementations. Section.5 discussions the conclusion for proposed PV central/string architecture.

2. LITERATURE SURVEY RECENT STUDY

Uniform irradiance is give higher outcome, but the non-uniform irradiance significantly lowers level then the power output of a Solar-PV array. The mismatching power losses on PV system are depends on shading pattern, physical location of modules, and PV array structure

everything have an impact on PV power output reduction factor. Fig. 2 (a) depicts as PV array/string module with protected by bypass diode. Reconfiguration procedures are frequently employed to mitigate the effects of partial shading conditions [14].

The proposed research seeks to develop a hybrid intelligent algorithm for solar-PV systems that would enhance efficiency in power point monitoring by avoiding partial shadow effects. By increasing the PV output power through using reconfiguration techniques the output power efficiency of the panel improved. In addition to that the literature survey and research gap explain about the uses of additional converters, MPPT controllers, and sensors leads to major problem in Solar-PV power generation [15,16]. As a result, there are two distinct approaches for reconfiguring DC-DC schemes that is isolated and non-isolated. Several non-isolated converter DC topologies were examined with the typical MPP algorithms, which is based on efficiency, construction, switching frequency, and losses as well as other relevant factors. Unfortunately, several factors such as light generation or PV current, series and diode reverse saturation current, shunt resistance, continuous diode ideality, and semiconductor energy band gap cannot be found in the manufacturer’s data sheet for altering the PV array models. A variety of simulated scenarios of BFT-MPP, which is confirmed by experimental setups,

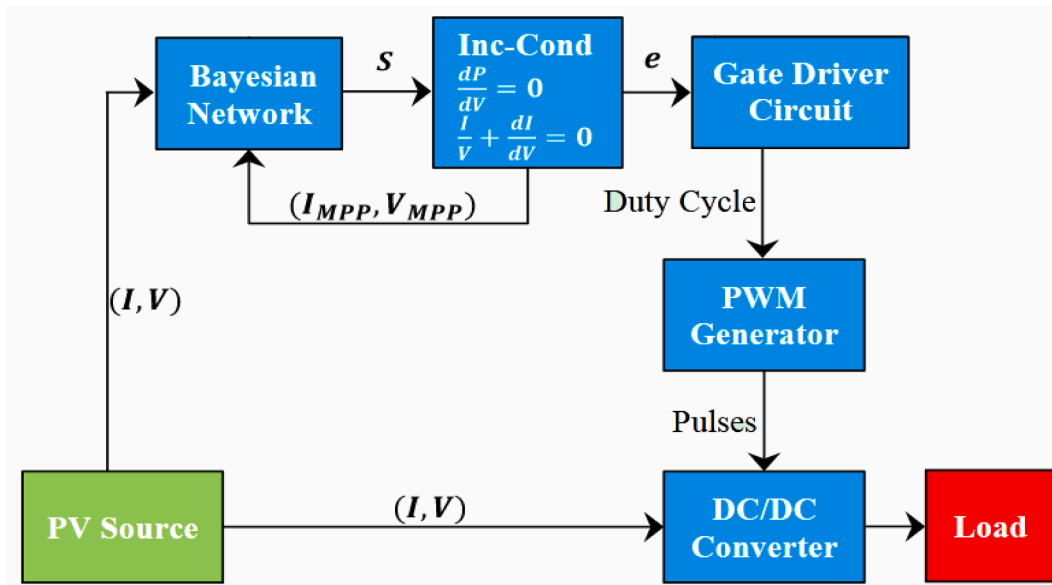


Fig. 2b. Proposed controller block diagram.

Table 1b  
Comparison of MPP techniques and soft computing optimization techniques.

Soft Computing Methods										
MPPT Technique	Dependency of array	Sensor type			MPP Tracking speed	MPP Tracking accuracy	Efficiency	Circuit Type	Application Grid connected	Standalone
		T	I	V						
<b>Artificial -Based Soft Computing-MPPT Techniques</b>										
Bayesian Network	X	X	✓	✓	M	Me	H	✓	✓	✓
Nonlinear Predictor	X	X	✓	✓	F	H	H	✓	✓	✓
Fibonacci Search	X	X	✓	✓	F	M	M	✓	X	X
Fuzzy Logic Control	✓	X	✓	✓	F	M	H	✓	X	X
Artificial Neural Network	✓	✓	✓	✓	F	M	H	✓	X	X
Extremum Seeking	X	X	✓	✓	F	M	M	✓	X	X
Differential Evolution	X	X	✓	✓	F	M	H	✓	X	X
<b>Soft Computing-Based MPPT Techniques</b>										
Ant Colony Optimization	✓	✓	✓	✓	F	M	H	✓	X	X
Cuckoo Search	X	X	✓	✓	VF	H	H	✓	X	X
Chaotic Search	X	X	✓	✓	F	M	M	✓	X	X
Genetic Algorithm	X	X	✓	✓	F	M	H	✓	X	X
Practical Swarm optimization	X	X	✓	✓	F	M	H	✓	X	X
Grasshopper	X	X	✓	✓	F	H	M	✓	X	X
Memetic Slap Swarm Algorithm	X	X	✓	✓	VF	H	H	✓	X	X
Dynamic Leader-Based	X	X	✓	✓	VF	H	H	✓	X	X
Collective Intelligence										
Shuffled Frog Leaping and Pattern Search	X	X	✓	✓	VF	H	H	✓	X	X

T = Temperature, I = Current, V = Voltage, D = Digital, A = Analog, VF = Very Fast, F = Fast, H = High, M = Medium, L = Low

and the closed loop block diagram of proposed BFT controller shown in Fig. 2(b). As a result, a solar BFT-MPP with a non-isolated switching converter is feasible solution for all different loads, and soft computing based MPP techniques detailed literature shown in Table.1(b). Nowadays, the present PV constructions are experiential with PV string type and PV array central type architecture using many applications. Fig. 3a. is displayed that PV central architecture for proposed system. Fig. 3b. is depicted that PV string architecture for proposed system.

PV Multiple reconfiguration processes along with different strategies are examined in the analysis. Static reconfiguration techniques were used to analyze testing of two phase PV array. This configuration with its unequally irradiated PV array methodologies for 9X9 Total-Cross Tied PV (TCTPV) array under various PSC described. Modifying the physical position of modules in the TCTPV array while keeping their electrical connections is possible using Sudoku and advanced Sudoku patterns.

Intelligent hybrid-based optimization algorithms are developed to minimize partial shading losses throughout the entire array by evenly spreading shadow. In the absence of shading, the PV array's Power-Voltage (P-V) characteristics have only one maximum power peak, whereas partial darkness causes numerous peaks. In the case of global MPP tracking for PV array under situations of partial and uniform irradiance Bayesian network approach is recommended. First time, BFT-MPP technique is applied in proposed PV string/central architecture and Bayes rule to estimate. Which is suitable for converters to produce maximum output power. For a real-time controller that is more effective output power is observed. In this approach reaches multiple clever state-of-the-art BFT-MPP algorithms in terms of tracking effectiveness, robustness, and speed with the help GWO/FPA.

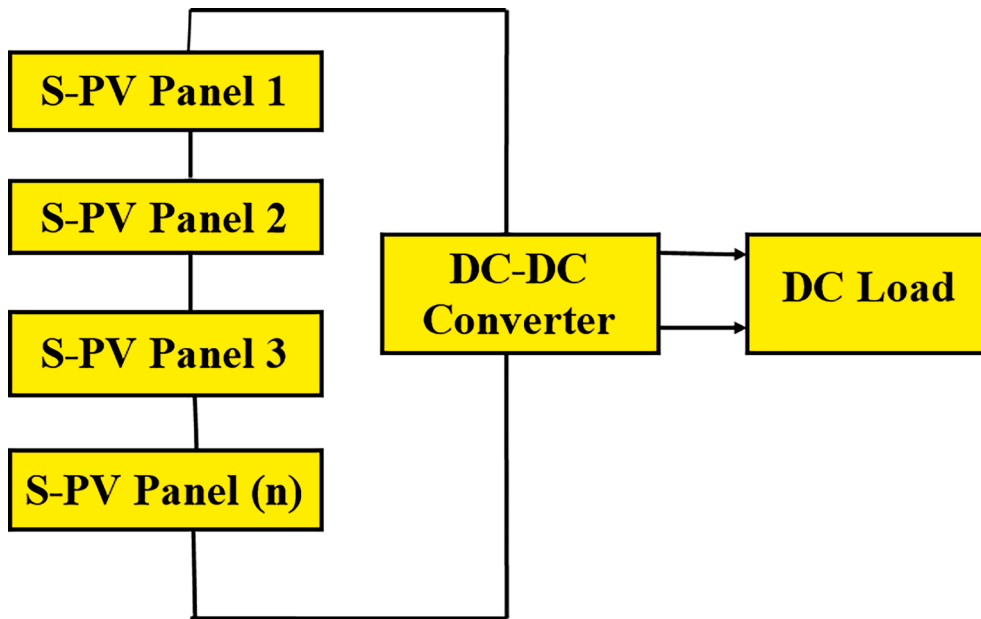


Fig. 3a. General architecture for central.

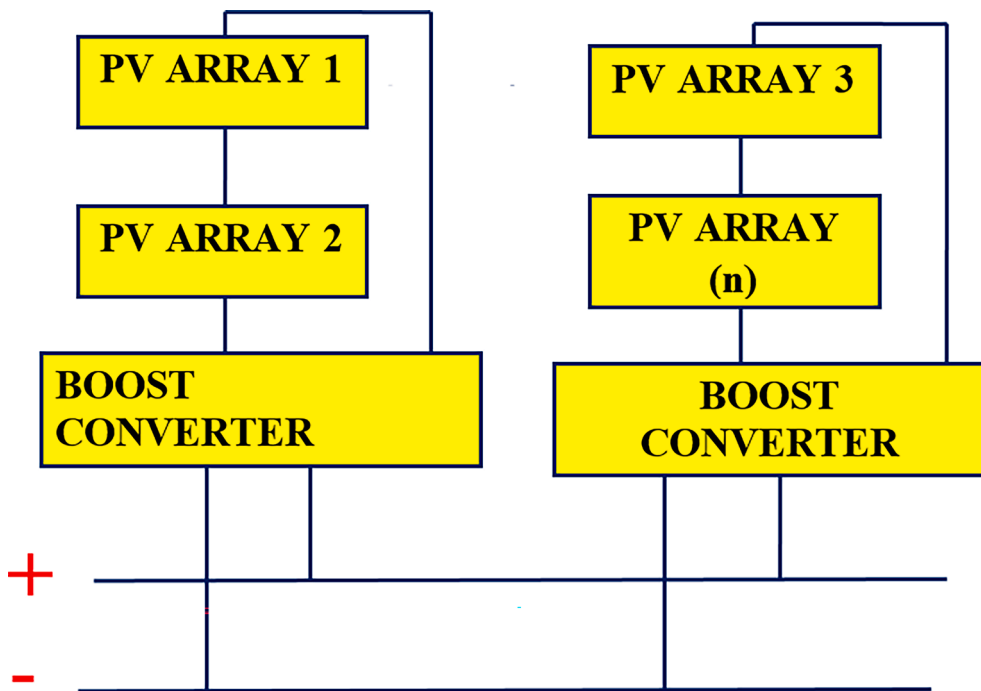


Fig. 3b. General PV String architecture.

### 3. Construction of proposed S-Pv panel

#### 3.1. Construction of S-PV PANEL

Under the different partial shading condition causes the current fluctuation from one panel to the next. It is challenging to capture the peak power. Since, PV panels generate lower output power. In order to solve this problem different types of architectural approaches are employed for achieving the maximum power. Out of all approach the PV central/string architectures provides better tracking efficiency and improved better Solar-PV panel conversion rate [17-20].

In this proposed work, four to twenty PV solar panels are arranged in

series connection, and the series connected PV panels output are given to converter. Then, it is connected to DC load as shown in Fig.3 (a). In this study takes into the account of six to twenty (n) number of PV panels are tested as illustrated in Fig.3 (b). PV array is categories into two strings, first one is PV string in each panel coupled with DC-DC converter. Which offers the peak power point tracking control for each individual string as presented. The PV string current of each solar panel with MPP is accompanied in between of the source and load [21-24]. As a result, the efficiency tracking in each PV string are higher than the central design under PSC condition [25].

Fig. 4 depicts as possible overall control PV structures for both the PV central/string array control (BFT-MPP) with FPA/GWO algorithm. The

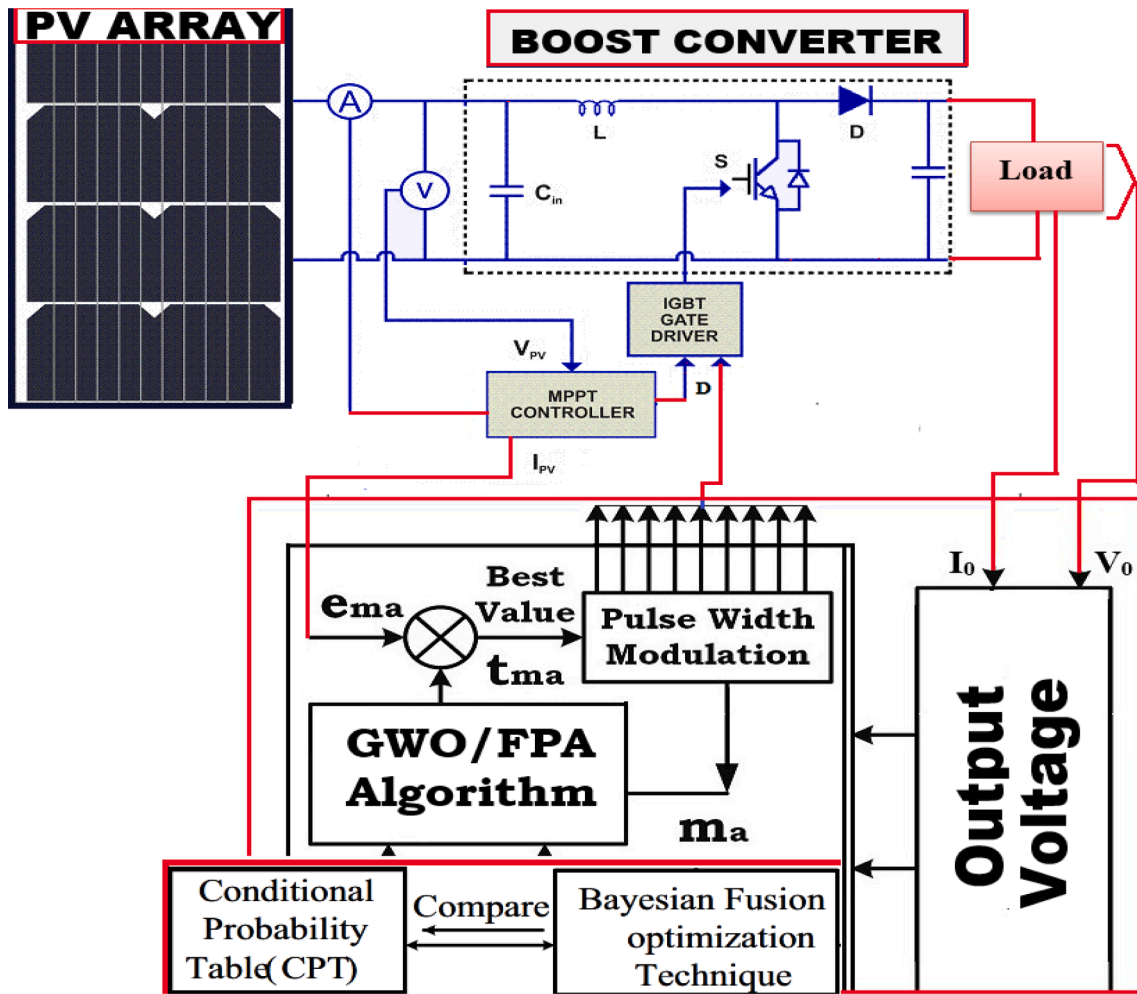


Fig. 4. Overall Circuit diagram for PV array control (BFT-MPP) with FPA/GWO algorithm.

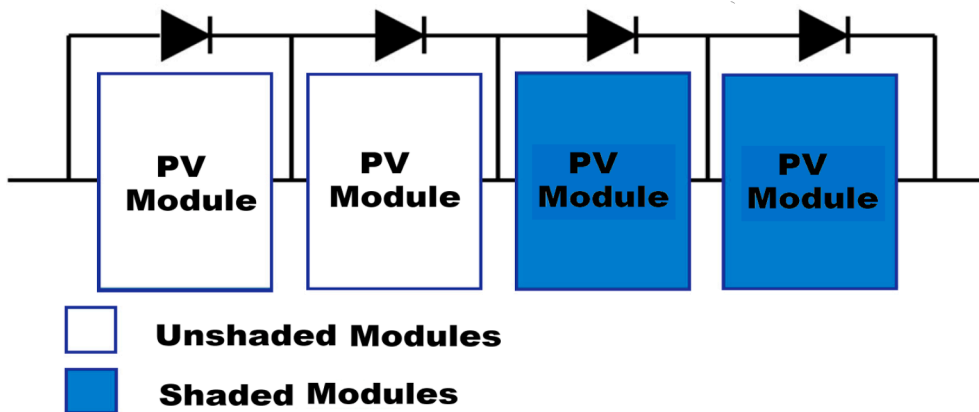


Fig. 5. Proposed shaded and unshaded PV module.

proposed DC converter operates for both the control circuit and power circuit. PV system control is used to operate the closed loop system. The reference output voltage and input voltage are found tuned with an optimization control method, hence that the execution results of duty cycle values under various irradiation situations are operated with help of the proposed optimization. Using four separate modules are 2 to 20 Solar-PV shaded/unshaded modules as shown in Fig. 5. The recommended system is previously implemented as an individual four (or) Six-module operational control output using various optimization

techniques. But proposed work implement up to 20 PV array modules are tested.

### 3.1.1. DC-DC converter circuit execution

Most of the solar PV system uses power (DC-DC) converters to change the voltage level from input source to load. These PV generated power is used to boost the voltage level with the help of DC-DC converter circuit [26]. The energy conversion of unshed PV systems is often to lower level voltage, and also exhibit the poor stability of unpredictable output

**Table 2**  
Traditional converter topology comparison.

Parameters	Converter Types		
	Buck converter	Boost converter	Buck-Boost converter
V <sub>out</sub> (output voltage)	V <sub>in</sub> D	V <sub>in</sub> 1/1-D	V <sub>in</sub> D/1-D
Number of Diodes	1	1	1
Number of Switches	1	1	1
Number of magnetic components	1	1	1
Efficiency	Low	Low	Moderate
Input ripple current	High	High	High

delivered in the (V-I & V-P) characteristics. Therefore, the MPP algorithm is necessary to make tracking the solar power in the entire PV architecture for both array type and central array architecture. Additionally, the converter achieves maximum output to compensate the load power and it's provides by the combination of MPP with different PV architecture. The main problem is affected solar-PV systems is the fluctuating availability of sun irradiation levels. Several power electronic DC-DC converters are used to overcome this challenge and maintain a consistent output voltage proportional to the load circuit.

The DC-DC boost converter is used to boost output voltage. It has a higher output voltage than the input voltage of the PV system. According to Fig. 4 shows that one kind of SMPS, which is minimum at least two type semiconductor switch addressed (transistor and diode). Therefore, one among the electrical energy storage device such as an individual

capacitor are ensembled of inductors (or) both it is used to generate the maximum output. In comparison of other converter circuits, conventional converter has a straightforward switching strategy that is not suitable to works with the proposed central/ string PV architectures.

To reduce output voltage ripple, the filter act as capacitor circuit are commonly involved to the DC-DC circuit, which is produce without any harmonics of the DC power. Therefore, proposed converter comparison as shown in Table.2. A theoretical calculation of boost converter output power = Converter input power- (P<sub>loss</sub> DC-DC converter).

Converter input power = S-PV array output power = 1450 W.

Therefore, Boost converter output power = (1450-40.13.) W.

Hence, Efficiency of the converter estimation = (1450-40.13)/1500 = 94%.

Boost converter power losses are calculate given by,

- (1) IGBT conduction loss, (2) IGBT Turn ON/OFF losses (3) Capacitance loss (input), (4) Capacitance loss (output), (5) Diode (D) loss, and (6) Inductor (L) loss.

• **Conduction loss**

$$P_{loss_{Ron}} = I_c^2 \times R_{on} \tag{1}$$

Where, Collector current is I<sub>c</sub> and Ron is resistance ON condition.

• **Turn ON/OFF Loss**

$$P_{loss_{trise,fall}} = \frac{1}{2} \bullet (trise + tfall) \bullet I_{RMS} \bullet V_{CE} \bullet F_{sw} \tag{2}$$

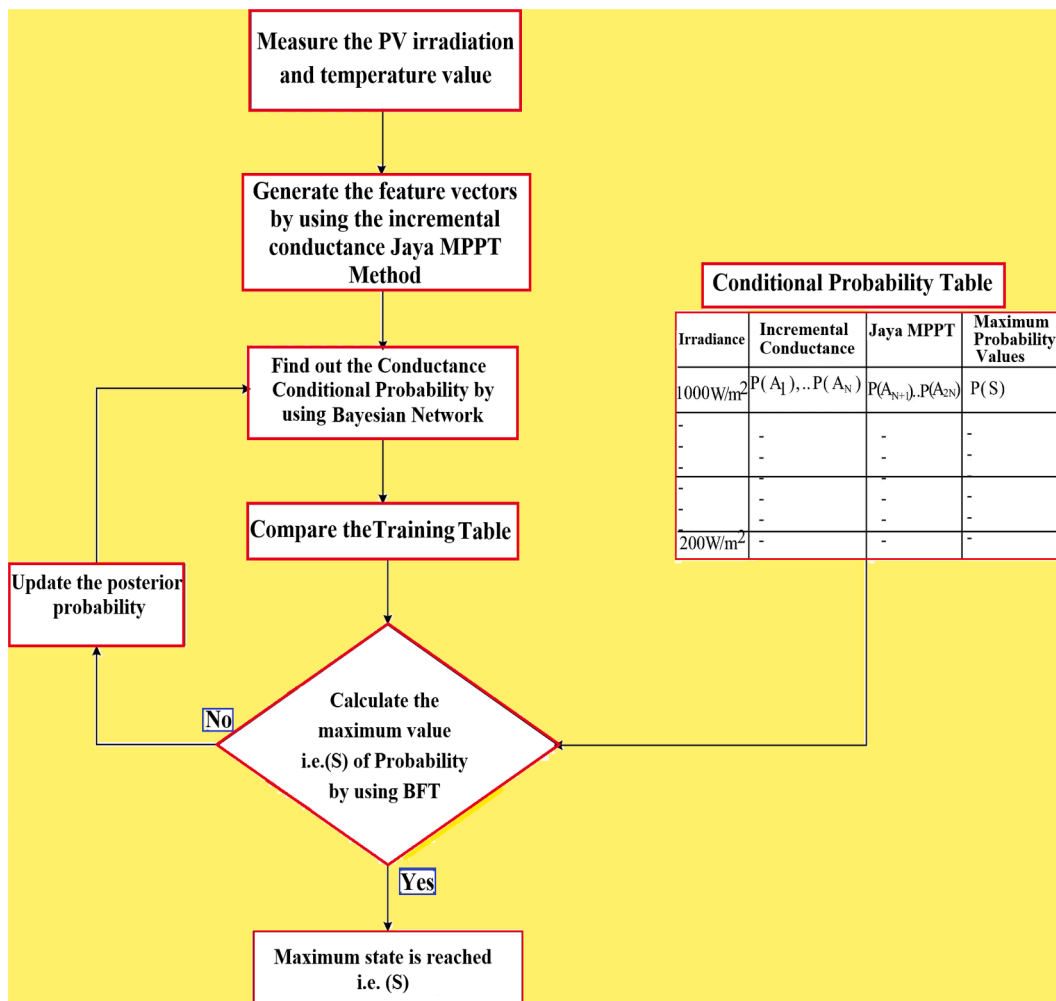


Fig. 6a. BFT-MPP Flowchart.

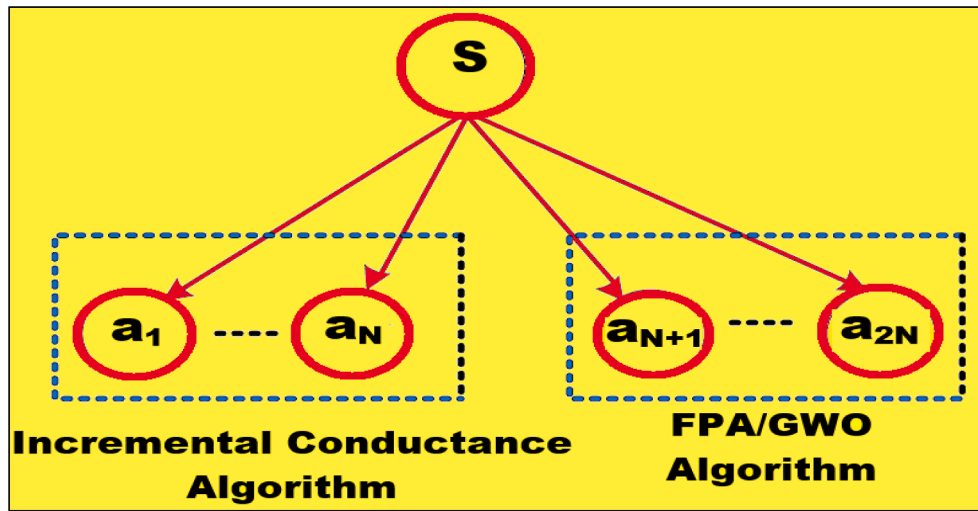


Fig. 6b. Structure using Bayesian fusion for MPPT data.

Where, rise time ( $t_{rise}$ ), fall time ( $t_{fall}$ ), RMS current ( $I_{RMS}$ ), Collector to emitter voltage ( $V_{CE}$ ), and Switching frequency ( $F_{SW}$ ).

• **Capacitance loss (Input)**

$$P_{loss\_gatecharge} = \frac{1}{2} Q_{gtotal} \cdot V_{GE} \cdot F_{SW} \quad (3)$$

Where,  $Q_g$  total is total gate charge,  $V_{GE}$  is applied gate to emitter voltage.

• **Capacitance loss (Output)**

$$P_{loss\_Coes} = \frac{1}{2} C_{oes} \cdot V_{CE}^2 \cdot F_{SW} \quad (4)$$

Where,  $C_{oes}$  is output capacitance of the IGBT.

• **Diode (D) Loss**

$$P_{loss\_diode} = I_{RMSDIODE} \times V_F \quad (5)$$

Where, RMS current through the diode ( $I_{RMSDIODE}$ ) however, forward voltage of the diode ( $V_F$ ).

• **Inductor (L) Loss**

$$P_{loss\_inductor} = I_{RMS\_INDUCTOR}^2 \times R_{DC} \quad (6)$$

$$\text{Efficiency} = \frac{\text{Output Power}}{\text{Output Power} + \text{Total Losses}} \quad (7)$$

$$\text{Duty Cycle} = \frac{T_{on}}{T_{on} + T_{off}} \quad (8)$$

• **Boost converter losses calculation:**

$I_{RMS}$  of IGBT =  $I_c$  of IGBT = 5A;  $R_{on}$  = 0.01  $\Omega$ ;  $t_{rise}(tr)$  = 68 ns;  $t_{fall}(tf)$  = 65 ns;  $V_{CE}$  = 230 V;  $F_{sw}$  = 10KHz;  $Q_g$  total=257nC;  $V_{GE}$  = 15 V;  $C_{OES}$  = 260pF;  $I_{RMS}$  diode value = 7A;  $V_F$  = 0.7 V, Inductor ( $I_{RMS}$ ) = 7A;  $R_{DC}$  = 0.1  $\Omega$ .

- $P_{loss_{Ron}} = 5^2 \cdot 0.01 = 0.2500$  W
- $P_{loss\_trise\_tfall} = 0.5 \cdot (68 \times 10^{-9} + 65 \times 10^{-9}) \cdot (5 \cdot 230) \cdot (10 \times 10^3) = 0.7647$  W
- $P_{loss\_gatecharge} = 0.5 \cdot 257 \times 10^{-9} \cdot 15 \cdot (10 \times 10^3) = 0.0193$  W
- $P_{loss\_Coes} = 0.5 \cdot 260 \times 10^{-12} \cdot 230^2 \cdot (10 \times 10^3) = 0.0688$  W
- $P_{loss_{IGBT}} = P_{loss_{Ron}} + P_{loss\_trise\_tfall} + P_{loss\_gatecharge} + P_{loss\_Coes}$

$$= 0.25 + 0.7647 + 0.0193 + 0.0688 = 1.1028 \text{ W.}$$

- $P_{loss}(\text{Diode}) = 7 \cdot 0.7 = 4.9$  W
- $P_{loss}(\text{Inductor}) = 7^2 \cdot 0.1 = 4.9$  W
- $P_{loss\_converter} = P_{loss\_diode} + P_{loss_{IGBT}} + P_{loss\_inductor}$

Hence, the converter losses ( $P_{loss\_converter}$ ) =  $4.90 + 1.1028 + 4.90 = 10.90$  W.

3.1.2. *BFT-MPP implementation*

There are several methods are presented to tracking the power in the S-PV system. The right size of a PV array system is the first step toward effective system utilization. The best usage of tilting and MPP is only significant after the best size selection. Because, the low initial investment through sizing. The suggested system also takes into account a number of additional factors, such as solar protection, energy conversion, source integration, and the use of MPP approaches for maximizing power extraction to the load. Maximum Power Point (MPP) tracking is an S-PV power converter algorithm that continuously modifies the impedance values[5]. Under varying environments condition like as changing the solar irradiance, temperature, consequently the solar array output in order to keep changing like peak power (or) low power point output to the load. The P&O (Perturb & Observe) and INC (Incremental Conductance) procedures are considered as usual. Since they have been used for many years. Therefore, we are presented BFT-MPP implemented in this proposed design. A Bayesian network is used to build the BFT-based MPP tracking approach.

A Bayesian network is a powerful tool derived from the Bayes theorem, which is used for statistics fusion with joint probability distributions. The BFT is trained using the training data set (input, output) shown in Fig. 6(a). Feature vector production is one among the segment of BFT process [27]. A Bayesian network is a statistical method that to make progress in obtaining Global MPP under the PV array PSCs. Based on the proposal, the proposed work was about the joint probability distribution of the fusion of data for using the FPA/GWO algorithms and incremental conductance. Much better to comprehend to visualize a PV system with six modules are observed. The linking series with an input on each PV module voltage and current combinations at 1500 W/m<sup>2</sup>, and the PV system's overall open-circuit voltage will  $V_{oc}$  must equal  $\eta V_{OCM}$ . At this point, a Bayesian network is created and observing nodes' inputs, i.e.  $L = a_1, \dots, a_n$ , which are equally split into the left and right nodes  $a_1, \dots, a_n$  (left nodes), and  $R = a_{n+1}, \dots, a_{2n}$ . Therefore,  $L =$  The left nodes  $a_1, \dots, a_n$  are given the individual panel voltage information, while PV are operating at MPP and incremental conductance in a partly

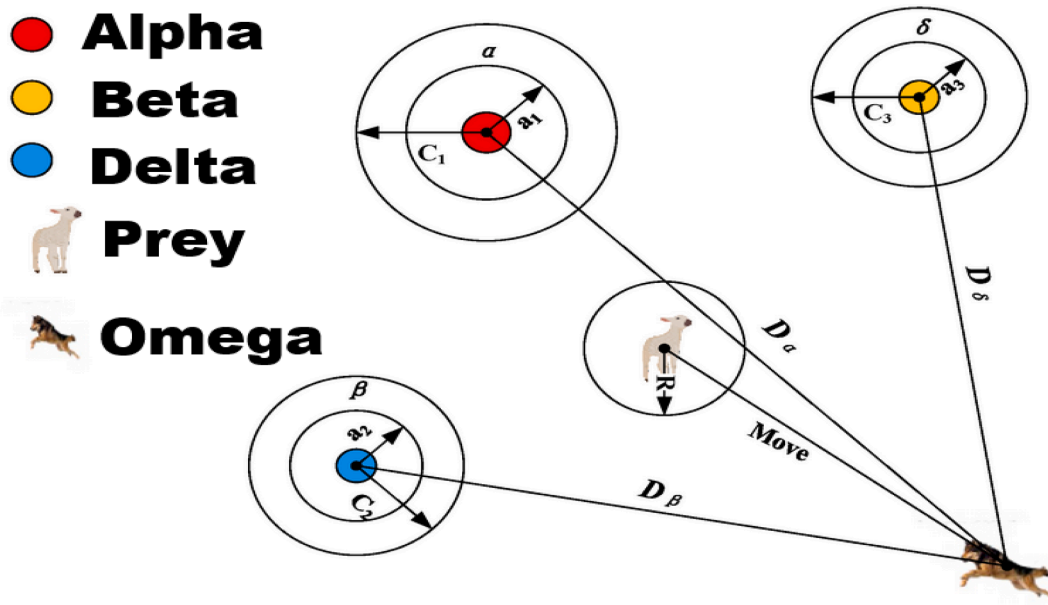


Fig. 6c. Position updating mechanism.

shaded environment [28]. In the same way, the right nodes  $R = a_{n+1}, \dots, a_{2n}$  are allocated using input voltages acquired across individual panels while the PV system is operating under comparable partially shadowed conditions and implementing the BFT-MPP algorithm.

Fig. 6(b) depicts the Bayesian network's network configuration. The posterior probabilities in Bayes theorem are determined by the prior probability distribution. The prior probability distribution is derived by statistical inference based on a set of prior knowledge. The posterior probability is calculated using the most recent system information and

the best reasonable evaluation. The prior probability is continually updated depending on the previous information provided, and the new posterior probabilities are estimated using Bayes' theorem. These posterior probabilities will aid in determining if the collection of information supplied is new event information or previous event information. Global Maximum Power Point (output) for both the FPA/GWO and incremental conductance methods are mentioned for each of the sample training data sets, which are input combinations of voltages and current pairs  $(V, I)$  of solar cell modules with varying irradiance and

```

Define the objective function  $\min f(x)$ ,  $x=(x(1), x(2), \dots, x(d))$ 
Initialize a population of n flowers/pollens gametes with a random solution
Find the best solution  $g^*$  in the initial population
Define a switch probability  $p \in [0, 1]$ 
t=1
while t ≤ Max Generation do
for i=1, ..., N do
if  $\text{rnd} \leq p$  then
Draw a (d-Dimensional) step vector  $L$  which obeys Levy distribution
Global pollination via  $X^i(t+1) = X^i(t) + L*(g^* - X^i(t))$ 
else
Draw from the uniform distribution  $\epsilon \in [0, 1]$ 
Randomly choose j and k among all solution
Do local pollination via  $X^i(t+1) = X^i(t) + \epsilon (X^j(t) - X^k(t))$ 
end if
Calculate  $(f(x(t+1)))$ 
If  $f(x(t+1)) \leq f(x(t))$  then
X(t) = x(t+1)
end if
end for
Find the current best solution of  $g^*$ 
t=t+1
End while
    
```

Fig. 6d. Pseudocode for GWO.

```

Initialize the grey wolf population  $X_i$ 
Initialize a, A and C
Calculate fitness of each individual in population
 $X_\alpha$ = the best solution
 $X_\beta$ = second best solution
 $X_\delta$ = third best solution
While (t< max number of iterations)
    for each wolf
        Update the position by equation 12
    end for
    Update a, A and C
    Calculate the fitness of all wolves
    Update  $X_\alpha$ ,  $X_\beta$ , and  $X_\delta$ 
    t=t+1
end while
return  $X_\alpha$ 
    
```

Fig. 6e. Pseudocode for FPA.

temperature[29]. Voltage, current, and matching output (GMPP) serve as the input data set. Eighty percent of the samples are chosen at random to serve as the training data set, and twenty percent of the samples are chosen to act as the testing set. If any two of the left and rightmost nodes match, "1" will be inserted in the feature vector; otherwise, "0." such that a(t) = designates feature a vector  $a_{1(t)}, \dots, a_{n(t)}$ . where,  $a_{i(t)}$  denotes the state of the  $i^{\text{th}}$  node at time t. For the purposes of simulation studies, a boost converter is used to link a PV system with four PV modules that are arranged in series to the freestanding loads. Table. 2 necessity display the boost converter's settings and data values for the proposed algorithms. The suggested Bayesian Fusion Optimization Technique (BFOT) is used to run the simulation and obtain the global maximum power point (GMPP) for different potential patterns in MATLAB/SIMULINK platform.

4. OPTIMIZATION APPROACH

Maximum power extraction under PSC is a significant difficulty for PV arrays and string operating condition. In this study, the optimization methods FPA and GWO are chosen to obtain the best optimum duty cycle for DC-DC converter to obtain MPP from PV array under PSC. The maximum power extraction under PSC is a minimum significant observed.

4.1. GWO optimization

Alpha ( $\alpha$ ), beta ( $\beta$ ), and delta ( $\delta$ ) are the three main leadership groupings among grey wolves. The alpha hunting mechanism as followed, which serves as the leader and decides everywhere to sleep. When the wolves get up in order to hunt for prey. The beta is required to abide by these rules. The beta wolf assumes leadership in the event that the alpha wolf passes away or matures.

The outcomes demonstrate that, in comparison to these well-known meta-heuristics, the GWO algorithm may deliver extremely competitive results. The following are the steps in the hunting process. Locating the prey, tracking the prey, and coming into contact with the prey as shown in Fig. 6(c).

Equations are used to update the wolves' positions as shown below:

$$d_\alpha = [C * X_\alpha - X], d_\beta = [C * X_\beta - X], d_\delta = [C * X_\delta] \tag{9}$$

$$X_1 = X_\alpha - [A * d_\alpha], X_2 = X_\beta - [A * d_\beta], X_{32} = X_\delta - [A * d_\delta] \tag{10}$$

$$X_{k+1} = \frac{(X_{\alpha_k} + X_{\beta_k} + X_{\delta_k} - \alpha(2 * rand - 1)[D_{\alpha_k} + D_{\beta_k} + DX_{\delta_k}])}{3} \tag{11}$$

$$D_{ik} = abs(2 * rand * X_i - X_k) \quad i = \alpha, \beta, \text{ and } \delta \dots \tag{12}$$

Where,  $d_\alpha$  is wolf position, 'rand' that is random number [0, 1],  $X_k$  is iteration (k) candidate position,  $X_{\alpha_k}, X_{\beta_k}, X_{\delta_k}$  is wolves position in iteration (k). Equ.9, 10 and 11 is updating the grey wolf position; Equ.12 is moment of wolf according to the GWO [30].

Fig. 6(d) illustrated as pseudo-code of GWO algorithms. GWO algorithms is used to initialize the parameters of PV panel irradiances level, after initializing the parameters the fitness population will be evaluated. Once the best solution has been found the maximum iteration will be stopped. Fig. 6(e) illustrated as pseudo-code of FPA algorithms. FPA optimization is used to initialize the switching probability parameters of PV panel irradiation levels; based on the maximum number of generation uniform distribution of random choice will be determined [31]. Once the best solution has been found, the maximum number of iterations will be stopped.

4.2. Fpa optimization

The primary function of a flower pollination reproduction is based on plant that produces cones. This is pollination like butterflies, birds, bats, and other animals carry eggs from one flower to another. The source of the worldwide pollination is shown below Eq. (13),

$$X_{i,n+1} = X_{i,n} + L(X_{i,n} - G) \tag{13}$$

Where, pollen 'i' is the current best solution among all solutions at the current iteration, 'G' is the best solution at iteration (n), and 'L' is the strength of the pollination, its value is given as,

$$L = \frac{\lambda \Gamma(\lambda) \sin(\frac{\pi \lambda}{2})}{\pi} * \left( \frac{1}{S^{1+\lambda}} \right) \tag{14}$$

The gamma function is  $\Gamma(\lambda)$  and  $\lambda$  value is Standard gamma function is  $\Gamma(\lambda)$  and  $\lambda = 1.5$ .

$$x_{i,n+1} = x_{i,n} + \varepsilon(x_{p,n} - x_{q,n}) \tag{15}$$

Where,  $x_{p,n}, x_{q,n}$  are chosen randomly that is same type of pollen plant from different flowers, therefore the  $\varepsilon$  value is [0, 1]. The FPA is used to determine the best duty (D) cycle of a group of flowers (N) as moves towards the best optimum values (G) [32]. Which is determined based on fitness variable that is observed maximum power from PV architecture [33]. By crating the MATLAB code that is iteratively appeal to Simulink PV model.

The FPA simulations are carried out to the entire iteration occupy the receiving parameters from the PV and its will analysis to sending the optimum duty cycle values. The best (D) optimum duty cycle is allocated in this search FPA optimization that remains in the  $K^{\text{th}}$  iteration process. Table.3(a&b) is portrayed as proposed algorithm parameter settings.

4.2.1. Algorithm steps for FPA

Steps of flower pollination algorithm are shown as follows,

**Step 1:** Activate N flowers for service and perform k optimization iterations.

**Step 2:** Make the fitness variable the maximum power  $P_{max}$ . Select the first  $P_{max}$ .

**Step 3:** Select the optimum switching angle and duty cycle determined as per fitness function of the algorithm as depicted as Fig. 7.

**Step 4:** Establish the upper and lower limits of the duty cycle.

**Step 5:** Establish a responsibility for each flower in step 5.

**Step 6:** To switch between local and global pollination, select a switch probability factor.

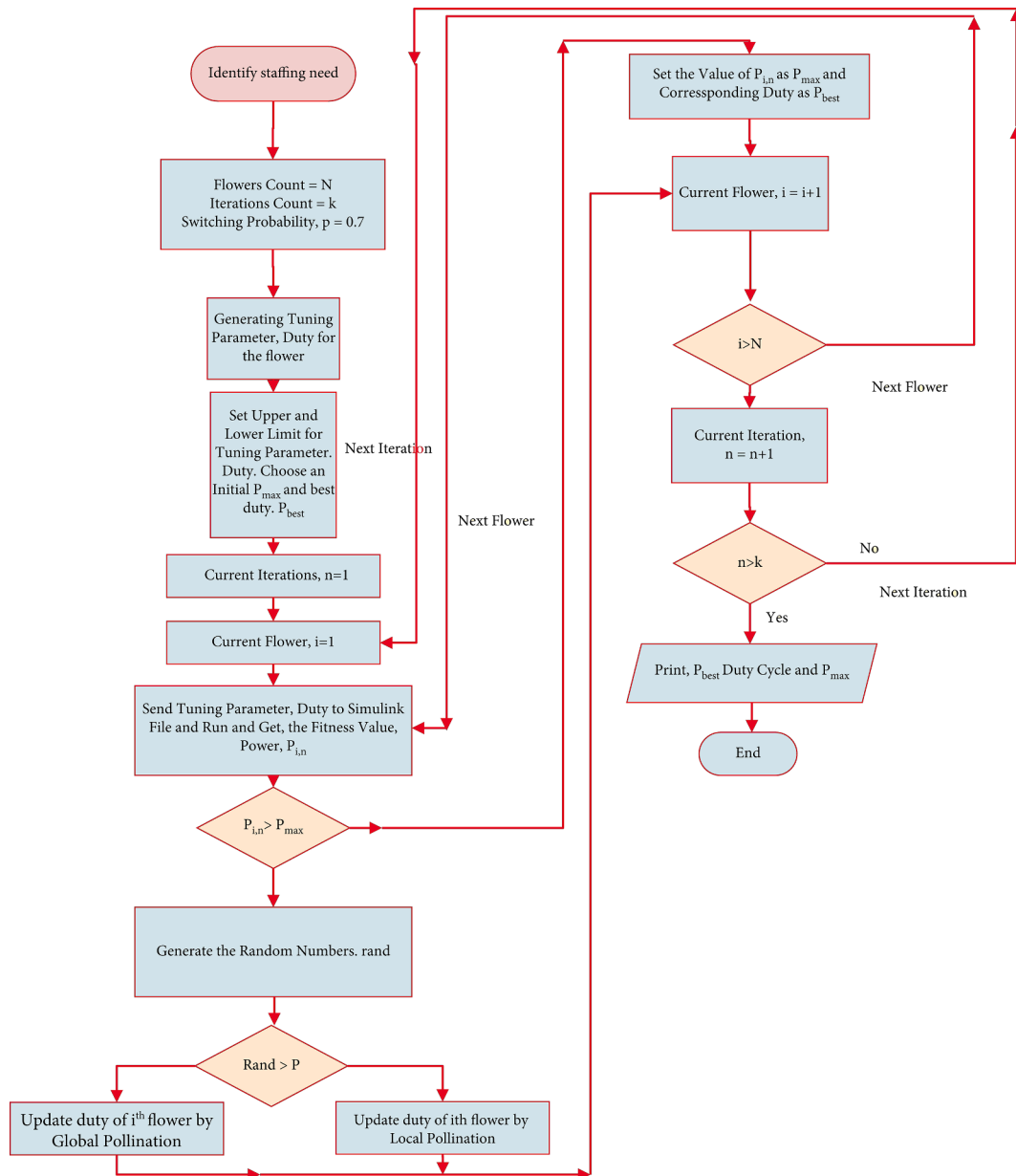


Fig. 7. Flowchart for FPA.

**Step 7:** Run the simulation using  $i$ th flower's  $n^{\text{th}}$  duty to obtain power  $P_{in}$ .

**Step 8:** Determine if  $P_{in}$  exceeds  $P_{max}$ .

**Step 9:** If the option is true (or) yes, therefore the set value is  $P_i$ , which is number ( $n$ ) at maximum responsibility of  $P_{best}$  solution gives to under every iterations method.

**Step 10:** If no means then random integer result should exceed then the switch probability factor, and select the global pollination (or) otherwise, if select the local pollination equation.

**Step 11:** Update the function of the  $i^{\text{th}}$  flower using the global (or) local pollination equation.

**Step 12:** To finish the iteration, repeat steps 1 through 6 for each flower individually.

**Step 13:** Improve the iteration count and carry out the aforementioned process  $k$  times.

**Step 14:** In all iterations, the  $P_{best}$  for duty and related  $P_{max}$  are changed.

**Step 15:** The optimal duty for maximum power is the value of  $P_{best}$  after ' $k^{\text{th}}$ ' repetitions.

#### 4.2.2. Algorithm steps for GWO

To increase the amount of power that a PV system can produce under PSC, the following processes are utilised to track the optimum PWM duty.

**Step 1:** Decide on a starting pack of wolves ( $N$ ) and the quantity of iterations ( $k$ ).

**Step 2:** Make the maximum power ( $P_{max}$ ) a fitness variable or an objective parameter.

**Step 3:** The Wolves' PWM responsibility is the key to achieving the goal.

**Step 4:** Determine the maximum and lower limits for the PWM duty cycle.

**Step 5:** Create PWM duty cycle.

**Step 6:** The sixth step is to generate the initial fitness function to each power of the wolf represented. Then, the rank of the wolf decreasing the order and assigns the top three parameters alpha ( $\alpha$ ), beta ( $\beta$ ), and delta ( $\delta$ ), To set the  $G_{best}$  duty cycle and the power equivalent is the obtained alpha as  $P_{max}$ .

**Step 6a:** Begin the  $n^{\text{th}}$  iteration by starting the simulation with each

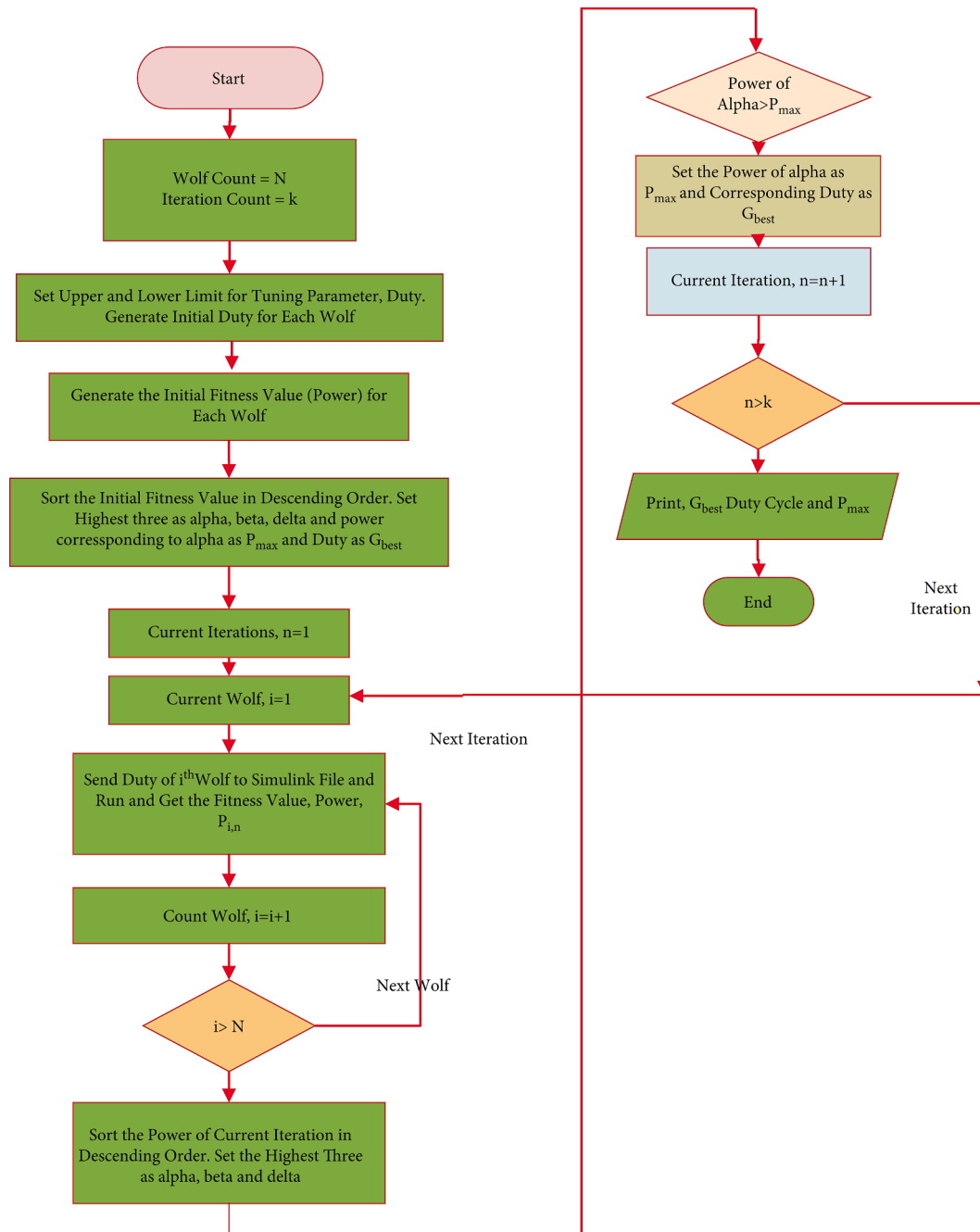


Fig. 8. Flowchart for GWO algorithm.

wolf's generate individually by the PWM duty pulse and verifying the power ( $P_{n,i}$ ) for the nth iteration for the all wolfs.

**Step 7:** Sort the power  $P_n$  in decreasing order using the letter 'i'.

**Step 8:** Use the top three highest powers to update the Alpha, Beta, and Delta.

**Step 9:** If the power associated with alpha exceeds  $P_{max}$ , set this power as  $P_{max}$  and the associated duty as  $G_{best}$  in the subsequent iteration.

**Step 10:** Calculate the difference between the current PWM duty cycle for Alpha, Beta, and Delta. So that the average of this difference may be taken in the following iteration.

**Step 11:** Displayed in Fig. 8, that is average value will be used to calculate the PWM duty for the.

Subsequent iteration.

**Step 12:** Rerun the upcoming iteration using the updated PWM duty

Table 3a

Proposed algorithm parameter settings.

Parameters for optimized Algorithm		
Specifications	GWO Data	FPA Data
Maximum iteration number	50	100
Number of Decision Variables	5	-
Population size	10	50
Switching Probability	-	0.8
Stopping Criteria	100 iterations	200 iterations

cycle.

**Step 13:** PWM duty cycle in Table.3(a) it shows that proposed algorithm of parameter settings with maximum iteration. and it is updated after the maximum iterations. Table 3b. shows that PWM duty cycle for

**Table 3b**  
Proposed BFT-MPP algorithm parameter.

Particulars	Specifications
Bayesian Fusion	Total data set = 528, training data = 81% of 528 (422), testing data = 21% of 526 (107)
Boost converter	$L = 5.21 \text{ MH}$ , $C_1 = C_2 = 10 \text{ }\mu\text{F}$ , $f = 10 \text{ KHz}$ ,
Incremental conductance	$D \text{ initial} = 0.16$ , $\text{Delta } D = 0.0052$
Sampling period ( $T_s$ )	For simulation, $T_s = 0.0024 \text{ Sec}$ .

**Table 4**  
Specification of PV panel.

Descriptions	Values
Rated power of PV panel (W)	400 W
Panel Short circuit current ( $I_{sc}$ )	20A
Panel Open circuit Voltage ( $V_{oc}$ )	20 V
Irradiance ( $\text{W}/\text{m}^2$ )	1500 $\text{W}/\text{m}^2$
Current at Maximum Power ( $I_{mp}$ )	16A
Number of cells per modules (n)	24

sampling period of proposed PV string/central architecture.

**Step 14:** After 'k' iterations, last iterations are halted. Gbest's value following the end of the 'k' iterations.

**5. EXPERIMENTAL/SIMULATION RESULT & DISCUSSION**

Performance of the PV central/ string design is evaluated in this section using simulation model. For the suggested methods, MATLAB files for analysing the FPA and GWO algorithm coding were formed. In order to determine the converter's total duty cycle and obtain the peak power under PSC circumstances, the proposed GWO/ FPA is created.

Table. 4 displays the solar panel and suggested simulation settings. The design and implementation of uniform/PSC irradiances for PV string unit was performed using Matlab/Simulink 2020a software. In this versatile software used to study about the dynamic irradiance level by using BFT-GWO/FPA optimization techniques. The optimization techniques were integrated in control unit, which is adopted with PV string (or) PV Central unit. Based on the different irradiances level voltage and current has been generated in the PV panel and it was sensed by current and voltage sensor. The bayesian fusion technique is used to

combine probabilistic models of different types of sensor data to provide a more comprehensive view of a particular environment. This BFT techniques incorporated with GWO/FPA optimization that is used to find the best solution of maximum power generation. According to the BFT-MPP techniques, the converter gate duty cycle has been varying proportional to the output power [33].

The simulation model of central architecture shown in the Fig. 9. Fig. 10 shows that PV characteristics of GMPP under PSC with comparison of existing network model. Fig. 11 demonstrates that the GWO simulation results for uniform irradiances that the power is taken from the PV array with no shadow conditions, which gives the power outcome 1450 W. When there is a shaded panel only 827.3 W of electricity is gathered, it is made up of four PV panels linked in series connection with a converter duty cycle 0.9. The boost converter outputs are lined to the DC load. The constant fixed STC temperature in all four PV panels is 25 °C. In each PV panel has different irradiation rate ranging from 1500  $\text{W}/\text{m}^2$  to 500  $\text{W}/\text{m}^2$ . The number of iterations in this simulation was described 200 for FPA and 100 for GWO algorithms. The number of wolves, population size is 10, and the simulation results are produces without any significant.

Fig. 12 shows that FPA simulation outcome PV array under uniform irradiance power is raised up to 1300.5 W at the time  $t = 2.8 \text{ sec}$  as shown in Fig. 12(a), Fig. 12 (b) depicted as converter duty cycle is value of 0.68, Fig. 12(c) shows that fitness value of the proposed algorithm at the value of 1246, and Fig. 12 (d) illustrate the maximum output power. In the FPA convergence period is longer than GWO and it is never move towards the steady state values. The FPA algorithm given in optimum duty cycle value is 0.6. Fig. 13 depicts as FPA MATLAB/simulation results that central architecture under shading conditions. The PV power irradiance value is 1000 W, the duty cycle converter is 0.8, the fitness value of the iteration is 1000, and the output power reveals that the FPA simulation utilizing PV string architecture under PSC is 1003 W.

The GWO simulation under shaded condition makes use of central architecture depicted as Fig. 14. PV array power output is 1090 W at the time  $t = 0.16\text{sec}$  as illustrate in Fig. 14(a), Fig. 14(b) shows that converter duty cycle is varied up to 0.3 to 0.9, Fig. 14(c) illustrate fitness function value is 1009, Fig. 14(d) shows that maximum output power is 1006 W. The GWO simulation under shaded condition makes use of PV string architecture depicted as Fig. 15. PV array power output is 1190 W at the time  $t = 0.12\text{sec}$  as illustrate in Fig. 15(a), Fig. 15(b) shows that converter duty cycle is varied up to 0.21 to 0.6, Fig. 15(c) illustrate

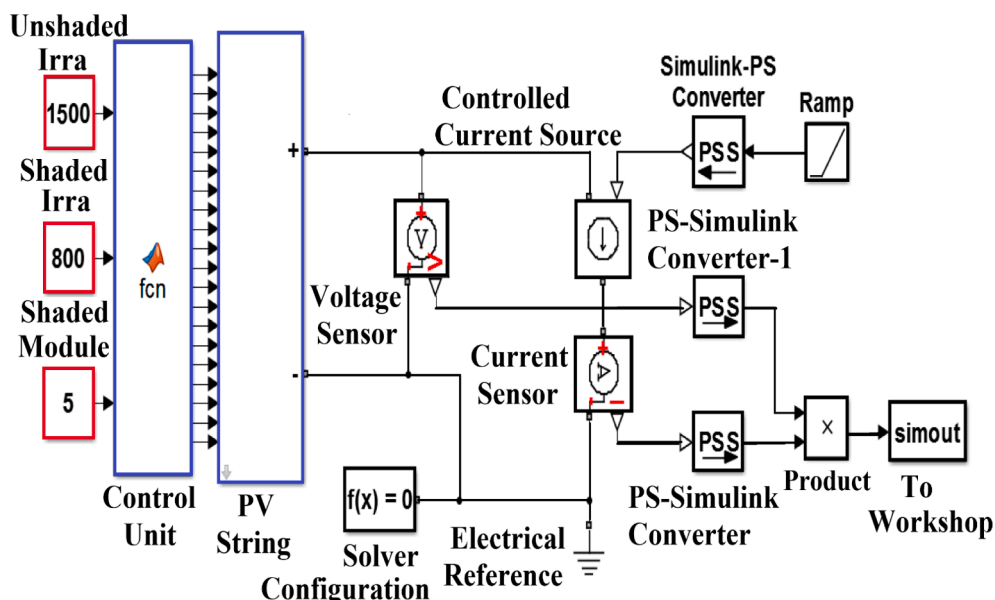


Fig. 9. Matlab Simulink model of PV string architecture with uniform/PSC irradiance.

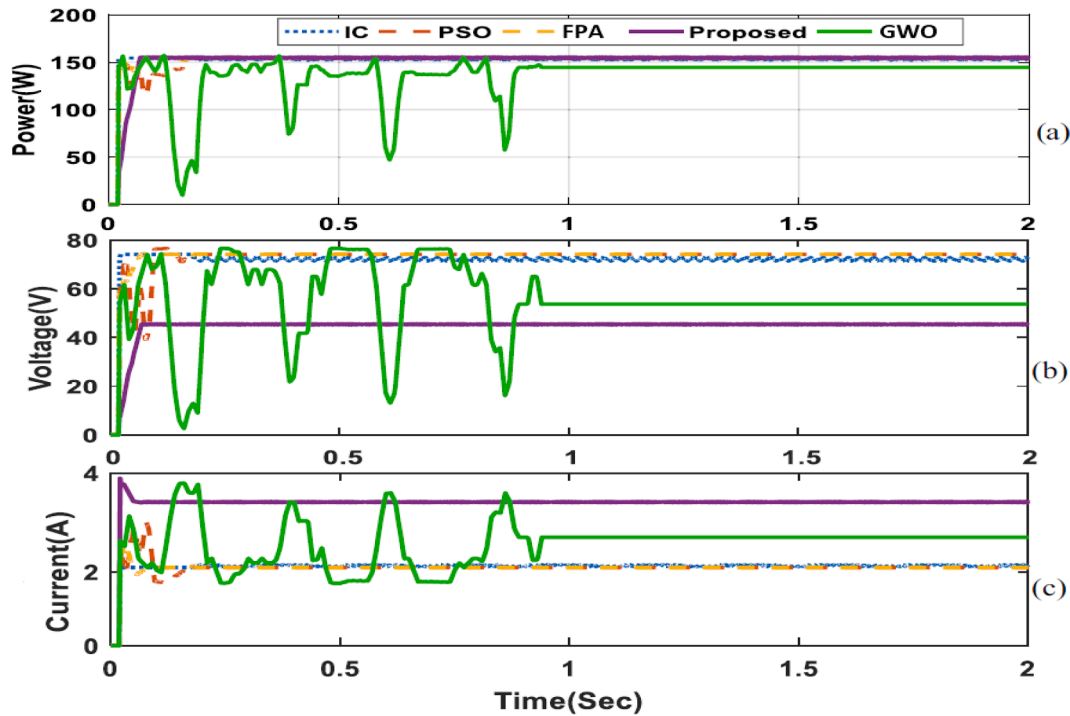


Fig. 10. Comparing Global MPP under PSC PV-array output.

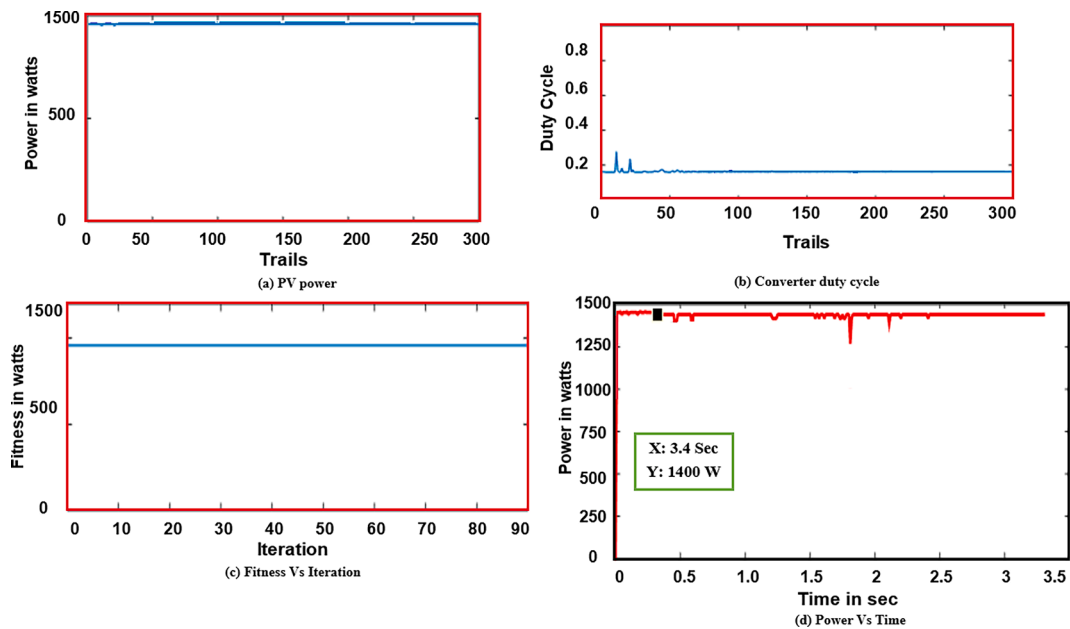


Fig. 11. GWO Matlab output for uniform irradiance.

fitness function value is 1003, Fig. 15(d) shows that maximum output power is 1260 W. Proposed GWO simulation under uniform shading irradiation condition using PV string architecture as shown in Fig. 16. At the time of  $t = 0.57\text{sec}$ , the PV array module output is 1045 W, converter duty cycle is 0.3 to 0.59, the fitness value of the iteration is 1003, and the maximum output power is 1260 W.

Therefore, the outcome of the PV array is observed that the power achieves a steady state value at the time of  $t = 0.166\text{sec}$ . But, the FPA is not reaches a steady state value. For that reason, the maximum power of the PV array using GWO algorithm extract the maximum power and send it to the DC load is 799.5 W. The power obtained from the PV array

characteristics output is 830.5 W. In the PV string architecture each string consist of 2 or 4 PV panel irradiance values is observed  $800\text{ W/m}^2$  &  $1000\text{ W/m}^2$ . Fig. 17 depicted as PV String architecture using FPA under uniform irradiation conditions with various output performance analysis. The comparative analysis of the GWO/FPA results are displayed in Table. 5 and 6. It demonstrates proposed algorithms' measurement is prescribed outcome based solar performance results. For the load resistance values are presented in the simulation  $3.75\ \Omega$  and  $4.5\ \Omega$  correspondingly.

There are two strings in the total number of PV central/string structure, and it will join together in a parallel-series arrangement.

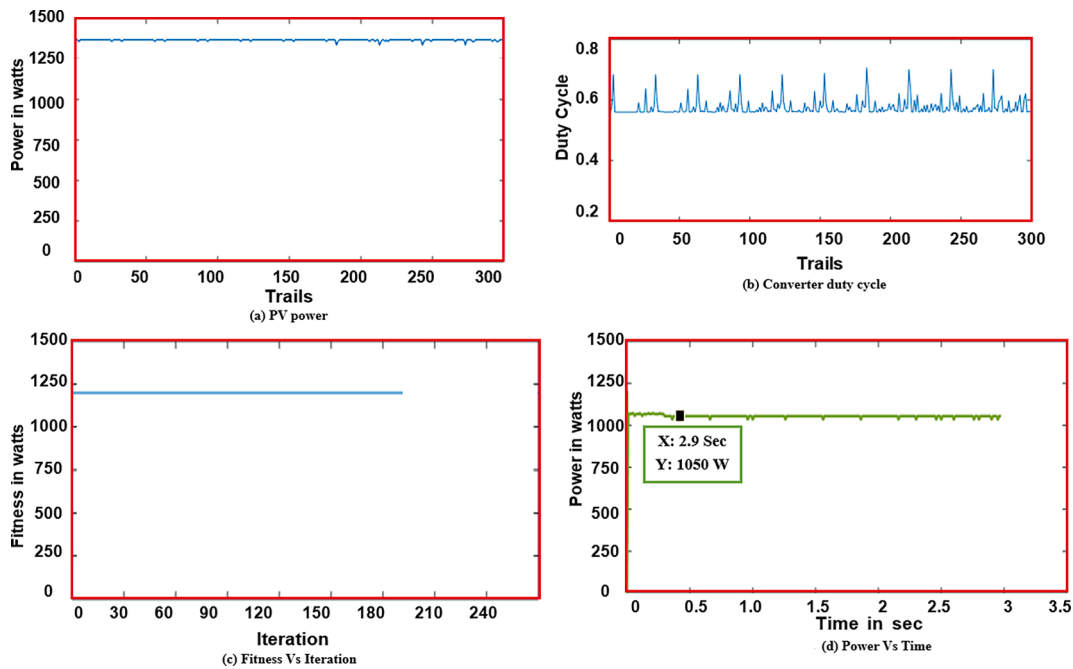


Fig. 12. FPA Matlab output for uniform irradiance.

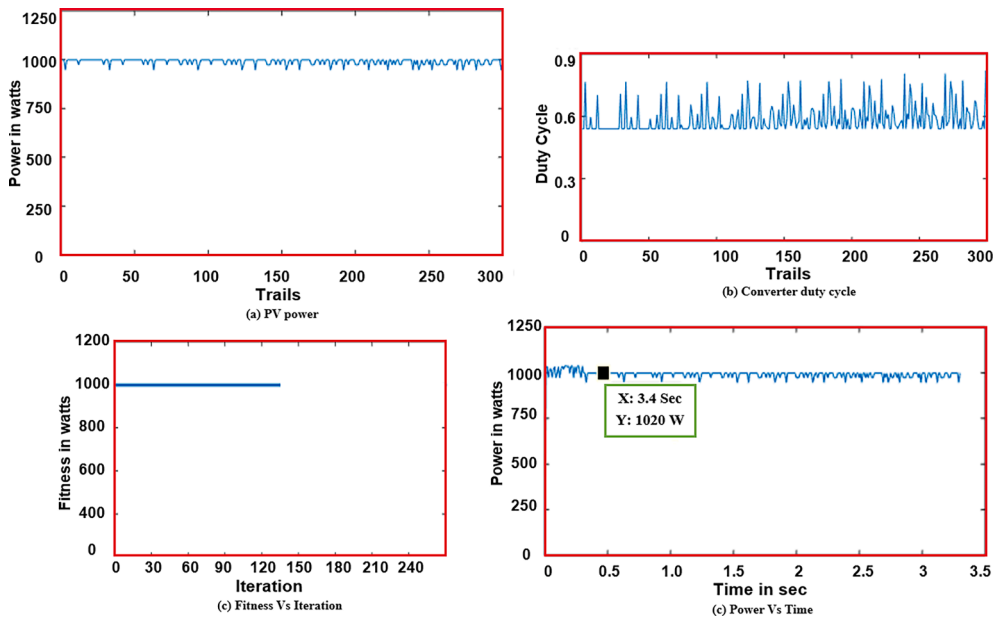


Fig. 13. FPA Matlab output for central PV configuration under shading conditions.

Outcome of the simulation of uniform and PSC using PV string architectures are shown in Fig. 18 (a, b, c, & d). Output power reach its maximum peak power of 829.4 W is shown Fig. 18 (a). At  $t = 0.56$ sec, the maximum output PV power reaches 959 W in the uniform irradiation conditions, and it's achieve steady state at  $t = 0.23$  sec. The BFT-MPP methods implemented into the proposed algorithms with two alternatives PV architecture are revealed in the literature and output results. Based on the study, which PV array design was best for maximum power transferring from PV source to load was established in this simulation test. Maximum power decreases by roughly 6.22% for every 200w/m<sup>2</sup> in the shaded module irradiance. When 20% of the PV array (String/central) modules are shaded under PSC irradiance falling in between 1200 and 800w/m<sup>2</sup>. However, the BFT-MPP only decreases by 0.25% for every 200w/m<sup>2</sup> in the shaded module irradiance between 800 to

zero. Fig. 19 (a&b) depicted as PV array configuration for proposed methods efficiency and fill factor values. When the shaded PV modules reach a crucial level of 700w/m<sup>2</sup> thus the solar PV array system is no longer sensitive to shading heaviness. Proposed PV system controller operating for both non-uniform and uniform PV array irradiance model is accomplished. Fig. 19 (c) compare to the convergence rates of several suggested optimization techniques. Fig. 19a. is depicted that proposed PV array fill factor values. Fig. 19b. is depicted that proposed PV array efficiency curve. Fig. 19c. shows that convergence rate of proposed hybrid optimization.

The real-time implementation of the PV array central architecture proposed in this research shown as Fig. 20. As well as, the same parameters of simulation and experimental data outcome results are observed and measured in Table 7 & 8. Fig. 19 (c) compare to the

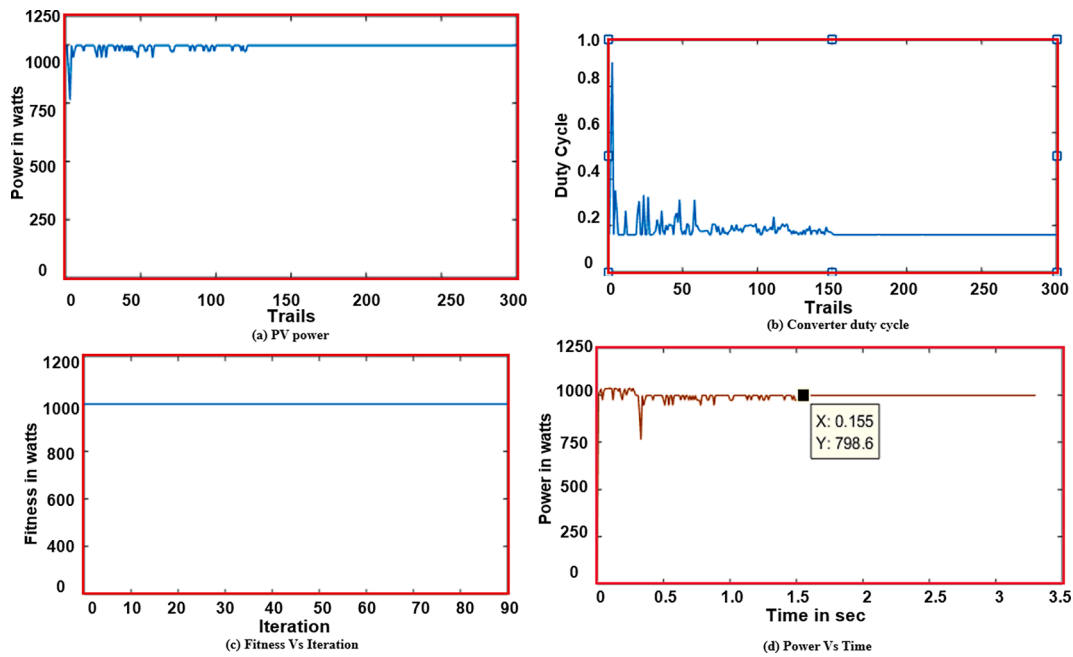


Fig. 14. GWO Matlab output for central PV configuration under shading conditions.

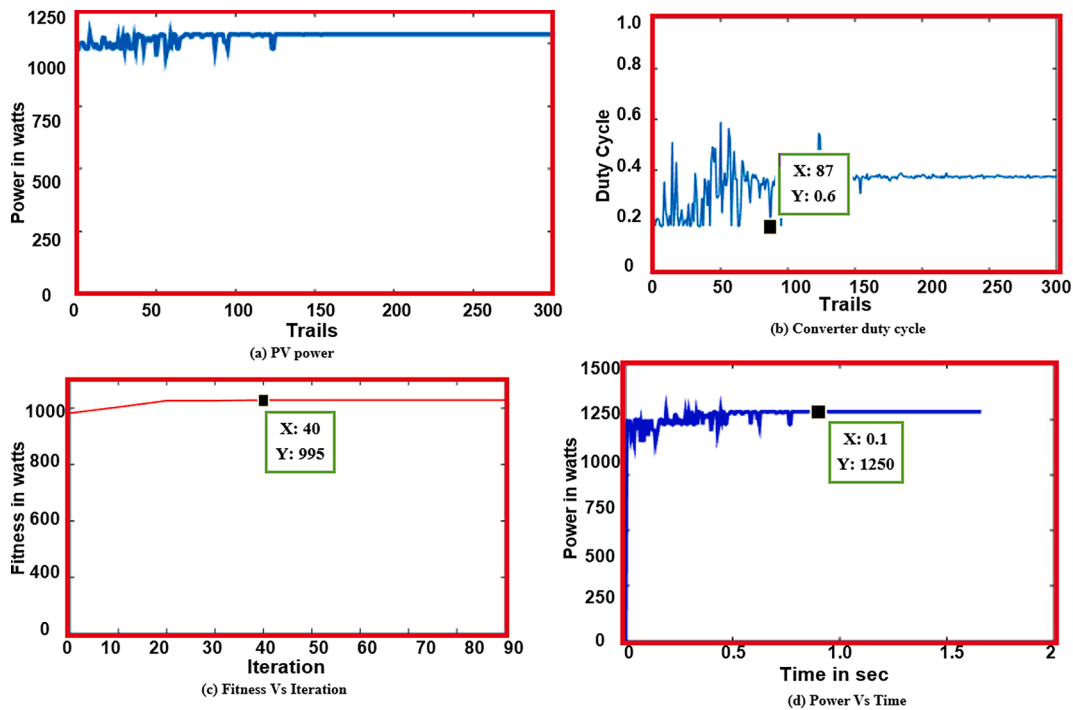


Fig. 15. GWO Matlab output for string PV configuration under shading conditions.

convergence rates of several suggested optimization techniques. Highest power generated by the load is 1450 W and it does not reach the steady state value depicted as Fig. 11. The outcome of the GWO simulation for the PV central architecture under the shading operating condition track the maximum power as shown in Fig. 14. For the Table.7 PV panel power is gained remarkably compared to other optimization techniques that is PV string architecture under uniform and partial shading condition compared with other existing methods. When compared to other optimization methods, the FPA has a better performance in achieving the steady state value. Therefore, the different PV structures with uniform and PSC are portrayed in Table.8. Which is PV central/string

architectures using PSC/Uniform shading condition compared with other optimization methods.

## 6. CONCLUSION

The performances of PV central/string arrays under various uniform, partial shading conditions were investigated using BFT-MPP optimization techniques. BFT-MPP techniques incorporate with traditional FPA and GWO methods were investigated in this research work. The proposed solar-PV to extract efficiently maximum power under various partial shading conditions. An attempt was made to prove this research

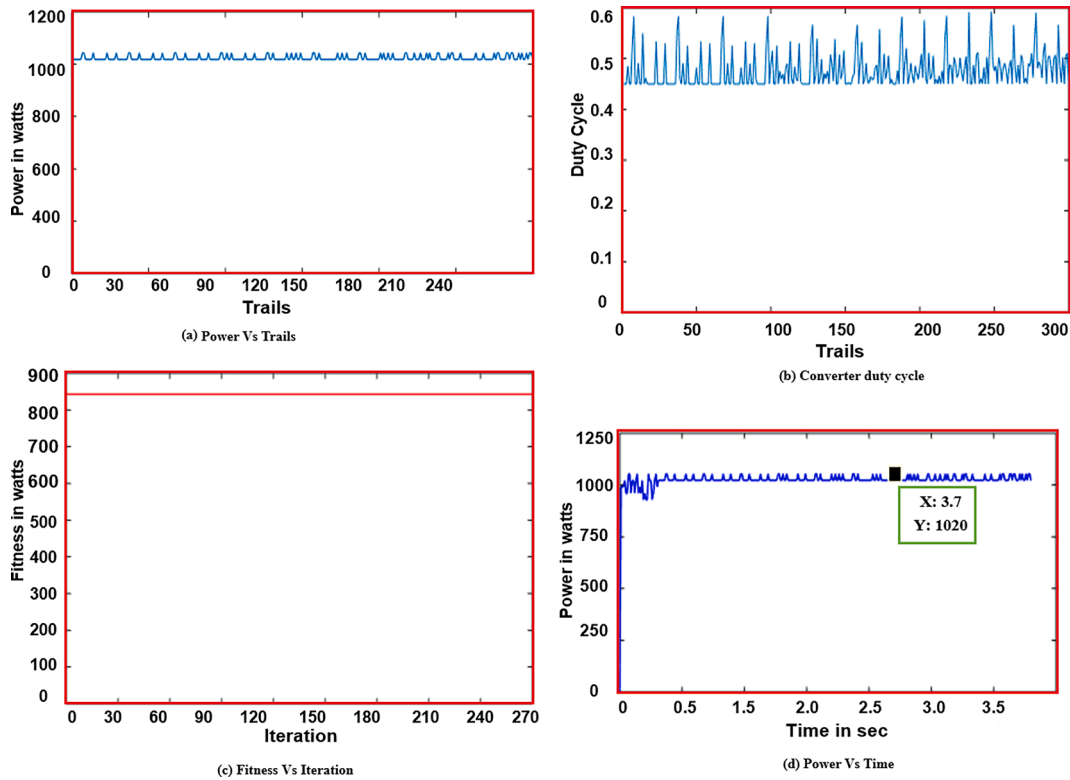


Fig. 16. GWO Matlab output for PV string configuration under shading conditions.

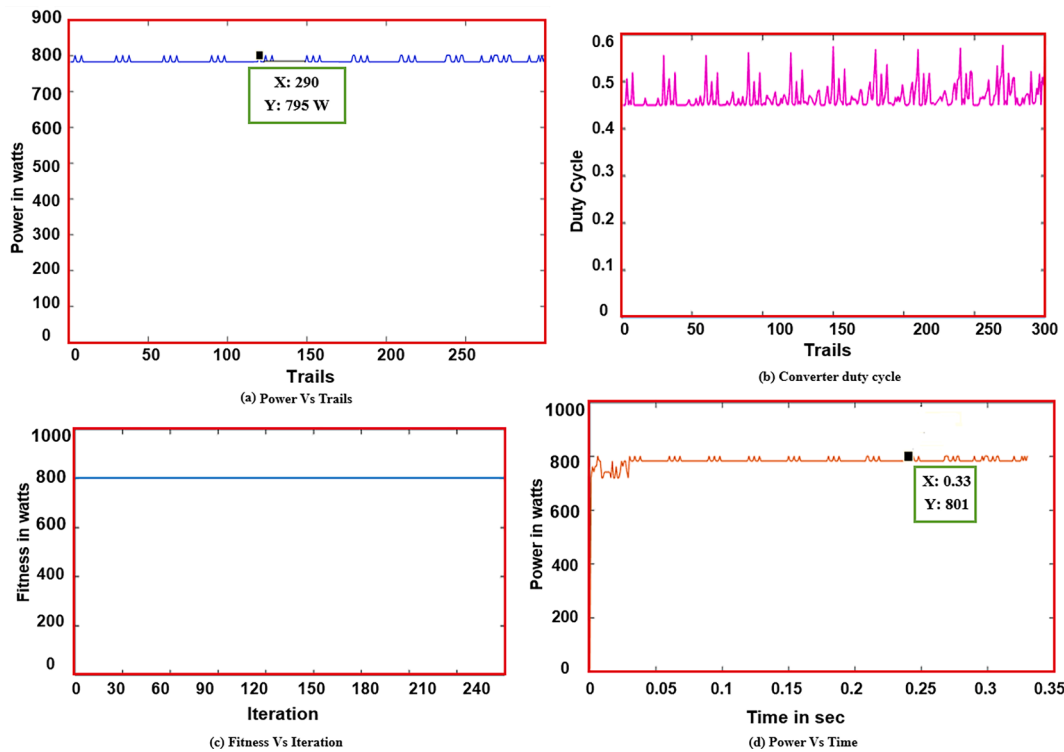


Fig. 17. PV String architecture using FPA under uniform irradiation condition.

using two analyses; (i) real time experimental data was collected from the PV panel. (ii) Simulation analysis using MATLAB/Simulink software have also conducted BFT-MPP based converter for central/string architectures under various partial shading conditions are performed. Results shows that, The GWO maximum tracking (MPP) power id 1450

W, and it is PV string design uniform irradiance tracking efficiency is 98.5%. PV string design maximum FPA tracking power is 1450 W and the tracking efficiency level is 96.3%. Similarly, the proposed PV central string architecture power tracking id 1050 W, and it is GWO based PSC produce the tracking efficiency of 98%. Over the FPA, which produce

**Table 5**  
Comparative analysis of simulation output measurements of central architecture PV.

S. NO	Max power (Pmax)	Algorithm types	$V_{pv}$ (V)	$I_{pv}$ (A)	$P_{pv}$ (W)	$V_o$ (V)	$I_o$ (A)	$P_o$ (W)	Conversion Efficiency (%)	Tracking Efficiency (%)
1	1360 W	FPA (In Uniform Irradiation conditions)	59.32	14.74	1051	59.43	13.04	1451	91.44	95.53
2	1461 W	GWO (In Uniform Irradiation conditions)	58.43	16.04	1321	59.43	15.02	1030	93.44	97.56
3	1000 W	FPA (In Central architecture)	57.32	18.04	1000	62.63	15.46	1062	94.44	98.56
4	1050 W	GWO (In Central architecture)	56.32	16.04	1201	63.02	14.72	1000	97.45	99.62

**Table 6**  
Comparative analysis of simulation output measurements of string architecture PV.

S. NO	Max power (Pmax)	Algorithm type	$V_{pv}$ (V)	$I_{pv}$ (A)	$P_{pv}$ (W)	$V_o$ (V)	$I_o$ (A)	$P_o$ (W)	Conversion Efficiency (%)	Tracking Efficiency (%)
1	1061 W	GWO (Shading condition)	56.32	13.04	1051	58.43	13.02	1251	94.44	95.56
2	1032 W	GWO (In Uniform Irradiation conditions)	58.43	14.04	1010	58.43	13.02	1020	95.44	96.56
3	852 W	FPA (In uniform architecture)	56.32	13.04	785	58.63	13.03	801	96.44	98.56
4	1250 W	FPA (Shading conditions)	57.32	14.04	1201	59.73	14.06	960	97.45	95.43

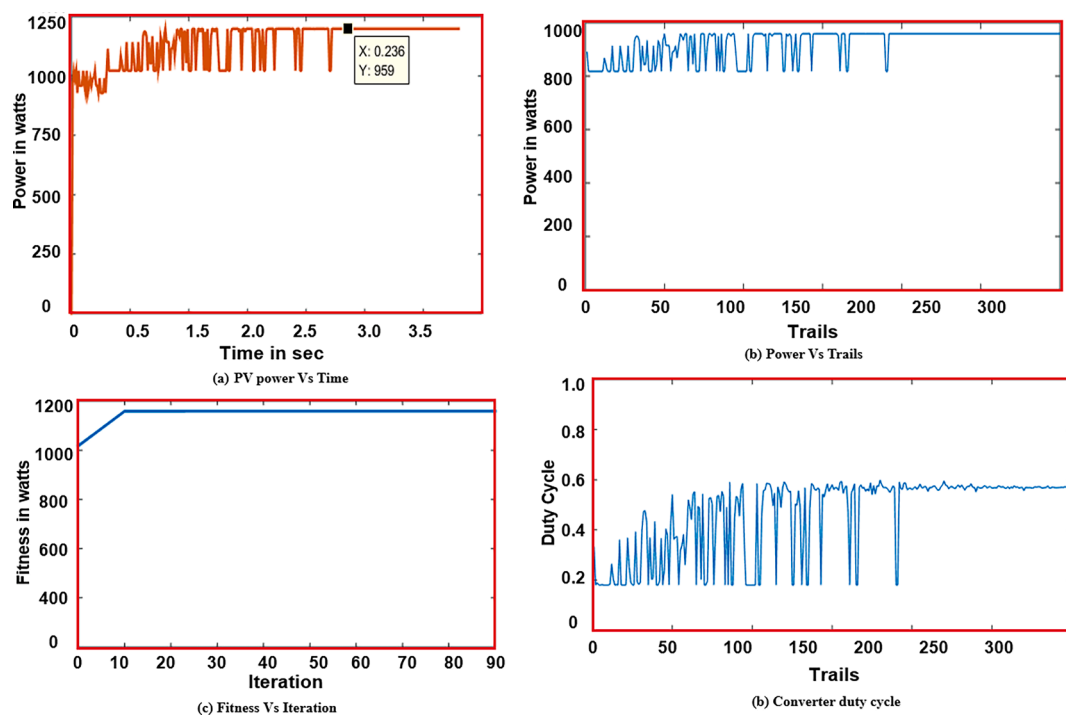


**Fig. 18.** FPA Matlab output for PV string configuration under shading conditions.

only 95% of tracking efficiency. Finally, GWO/FPA algorithm PV string gathers maximum power tracking from uniform/PSC irradiance achieve fast convergence rate compare to other existing methods. Upcoming researchers should further scrutinize this work for finding efficient way of extracting maximum power from solar PV panel at various partial conditions. Hence this work serves as open door for exploration of efficient way of extracting maximum power from solar PV power generation.

- Declaration & Conflict of interest
- Funding – The author did not receive support from any organization for the submitted work.

- Consent Statement – All authors mentioned have contributed towards the research work, drafting of the paper as well as have given consent for publishing of this article.
- Availability of Data & Material – The author hereby declare that no specific data sets are utilized in the proposed work. The have also agree to be accountable for all aspects of the work in ensuring that questions related to the accuracy or integrity of any part of the work are appropriately investigated and resolved.
- Consent to publication – all authors listed above have consented to get their data and image published

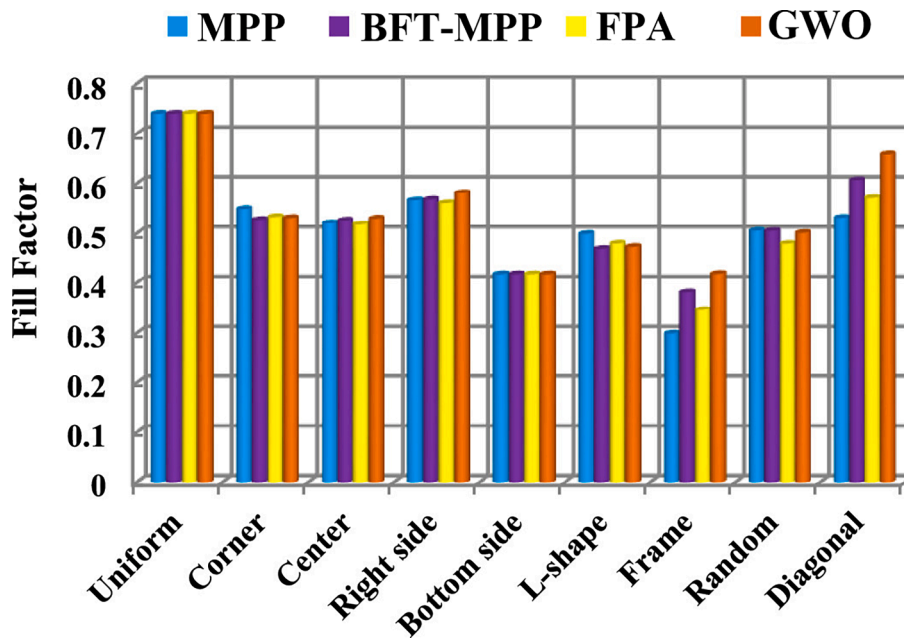


Fig. 19a. Fill factor for six PV array configuration.

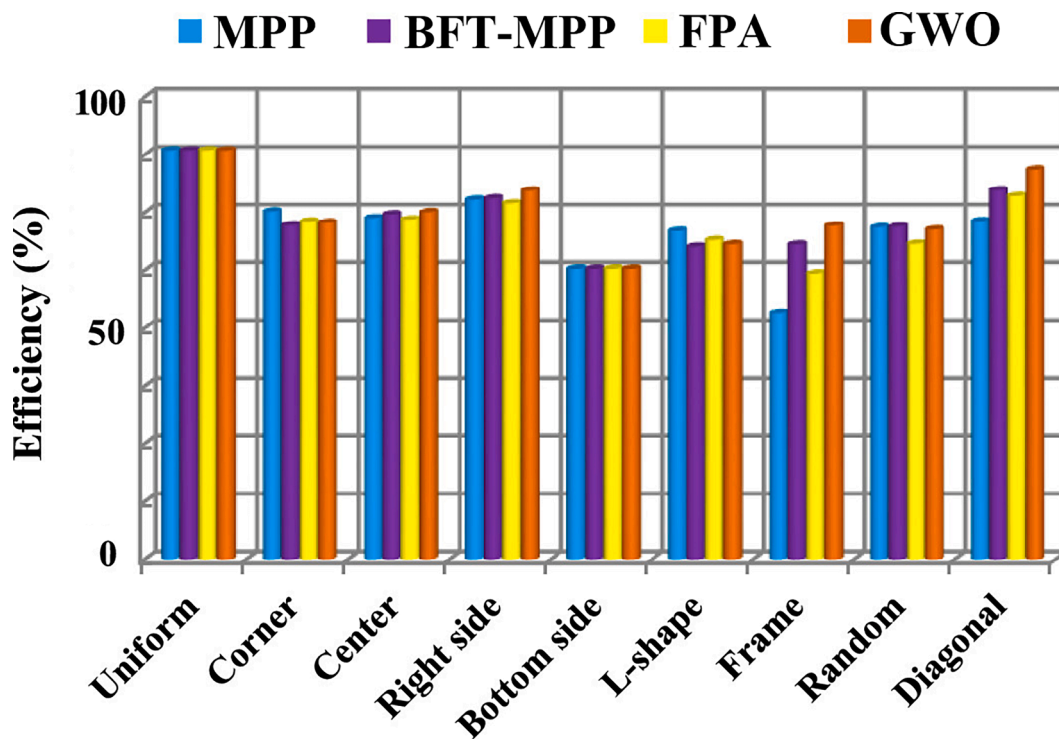


Fig. 19b. Efficiency for six PV array configuration.

- Code Availability – Since, future works are based on the custom codes developed in this work, the code may not be available from the author.
- The authors have no relevant financial or non-financial interests to disclose.

No Humans or Animals were involved in the experimentation.

- Conflicts of Interest - The author has no relevant financial or non-financial interests to disclose.

- Ethics Approval – The paper is an original contribution of research and is not published elsewhere in any form or language.

**Declaration of Competing Interest**

The authors declare that they have no known competing financial interests or personal relationships that could have appeared to influence the work reported in this paper.

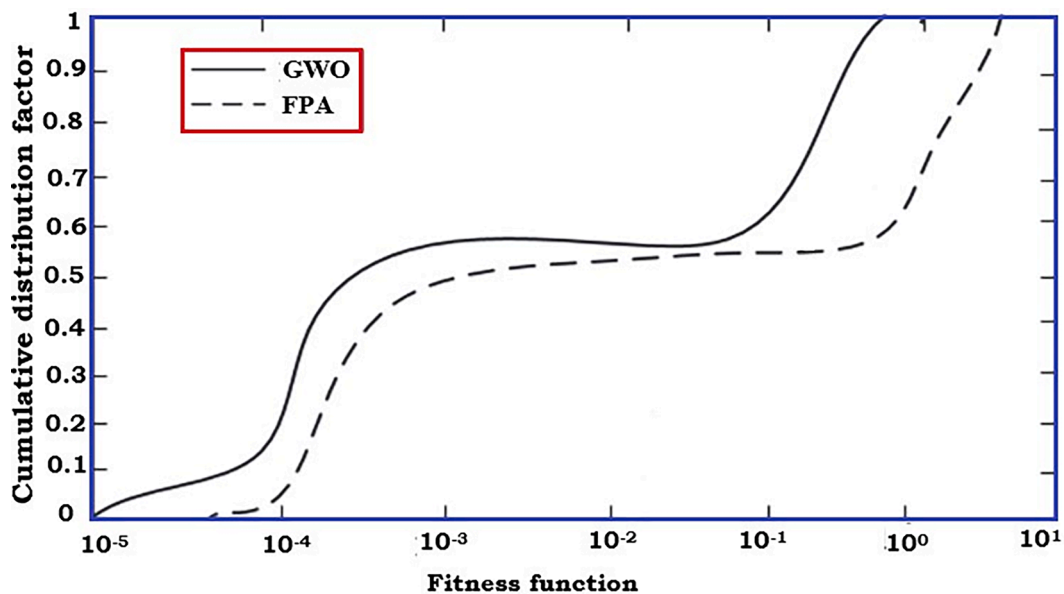


Fig. 19c. Convergence rate of proposed GWO & FPA optimization.

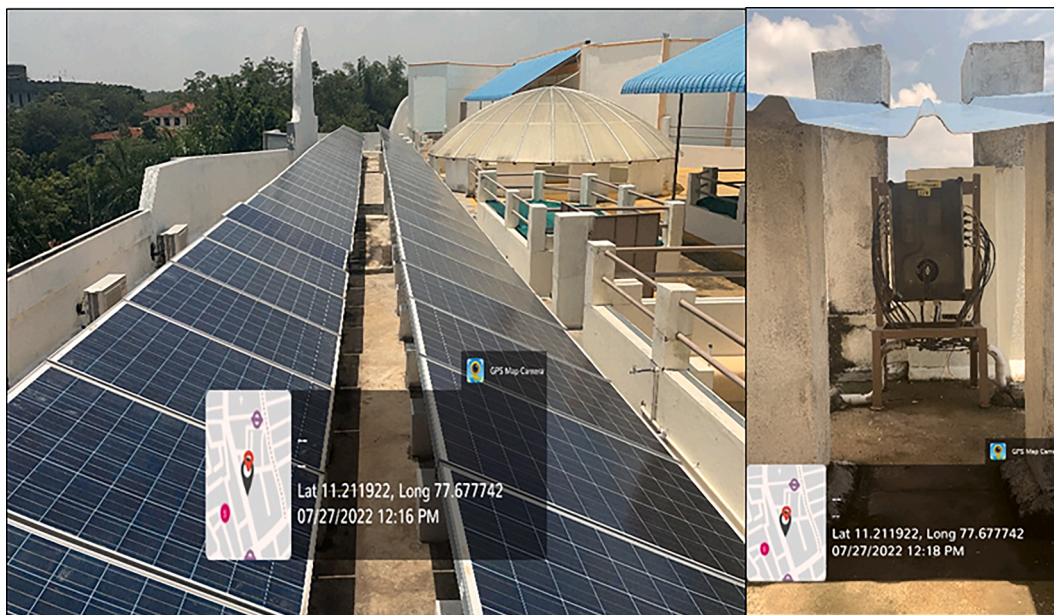


Fig. 20. Real time experimental PV array central architecture.

Table 7

Output measurements form PV string architecture under uniform and partial shading condition compared with other existing methods.

S. NO	Architecture	Algorithm type	$V_{pv}$ (V)	$I_{pv}$ (A)	$P_{pv}$ (W)	$V_o$ (V)	$I_o$ (A)	$P_o$ (W)	Conversion Efficiency (%)	Tracking Efficiency (%)	Irradiance Effect
1.	Existing PV-String [34]	BAT	51.1	11.6	1292	50	10.1	1121	86	86	
2.	PV string/ central [35]	FPA	49.1	10.23	1301	46	14.2	960	93.62	90.52	Uniform/ PSC
3.	PV string [36]	GA-FPA	47.01	11.81	1412	46.2	14.6	960	90.1	91	
4.	PV string [37]	GNN-MET	47	11.81		45	14.6	972	90.12	92.3	
5.		FPA	56.32	13.04	1051	58.43	13.02	1251	94.44	95.56	Uniform
6.	Proposed PV-String	GWO	58.43	14.04	1010	58.43	13.02	1020	95.44	96.56	PSC
7.		GWO	56.32	13.04	785	58.63	13.03	801	96.44	98.56	
8.		FPA	57.32	14.04	1201	59.73	14.06	960	97.45	95.43	

Table 8

Output measurements from PV central/string architectures using PSC/Uniform shading condition compared with other optimization methods.

S.NO	Max power (Pmax)	Architecture	Algorithm type	Convergence Time (sec)	Tracking Efficiency (%)	Irradiance
1	1350 W	PV- string/ central [38]	FPA	0.39	89	
2	1250 W	PV- central [39]	FPA	0.3762	91	
3	1350 W	PV-string [40]	FPA	0.1752	92.3	
4	1300 W	PV-string/ central [41]	MPP	0.1565	89	Uniform/
5	1200 W	PV-central [42]	MPP (P&O/INC)	0.892	90.9	PSC
6	1000 W	<b>Proposed PV-Central</b>	GWO	0.0319	95.56	Uniform
7	1050 W		FPA	0.0423	96.56	
			GWO	0.1553	98.56	PSC
			FPA	0.0476	95.43	
8	1450 W	<b>Proposed PV-String</b>	GWO	0.0235	86	Uniform
			FPA	0.2214	96.3	
9	1250 W		GWO	0.1825	98.5	PSC
			FPA	0.2452	90.52	

## Data availability

The data that has been used is confidential.

## References

- Teo JC, Tan RHG, Mok VH, Ramachandramurthy VK, Tan C. Impact of partial shading on the P-V characteristics and the maximum power of a photovoltaic string. *Energies (Basel)* 2018;11. <https://doi.org/10.3390/en11071860>.
- Youssef MAM, Mohamed AM, Khalaf YA, Mohamed YS. Investigation of Small-Scale Photovoltaic Systems for Optimum Performance under Partial Shading Conditions. *Sustainability (Switzerland)* 2022;14. <https://doi.org/10.3390/su14063681>.
- Gadiraju HKV. Improved Performance of PV Water Pumping System Using Dynamic Reconfiguration Algorithm Under Partial Shading Conditions. *CPSS Transactions on Power Electronics and Applications* 2022;7:206–15. <https://doi.org/10.24295/cpsstpea.2022.00019>.
- Albert JR, Stonier AA. Design and development of symmetrical super-lift DC-AC converter using firefly algorithm for solar-photovoltaic applications. *IET Circuits Devices Syst* 2020;14:261–9. <https://doi.org/10.1049/iet-cds.2018.5292>.
- Vanaja DS, Albert JR. An Experimental Investigation on solar PV fed modular STATCOM in WECS using Intelligent controller 2021;1–27. <https://doi.org/10.1002/2050-7038.12845>.
- Vanchinathan, K., Gokul, C., Albert, J.R.: An improved incipient whale optimization algorithm based robust fault detection and diagnosis for sensorless brushless DC motor drive under external disturbances. 1–25 (2021). <https://doi.org/10.1002/2050-7038.13251>.
- Murugesan M, Kaliannan K, Balraj S, Singaram K, Kaliannan T, Albert JR. A Hybrid deep learning model for effective segmentation and classification of lung nodules from CT images. *J Intell Fuzzy Syst* 2022;42:2667–79. <https://doi.org/10.3233/JIFS-212189>.
- Albert JR, Sharma A, Rajani B, Mishra A, Saxena A, Nandagopal C, et al. Investigation on load harmonic reduction through solar-power utilization in intermittent SSFI using particle swarm, genetic, and modified firefly optimization algorithms. *J Intell Fuzzy Syst* 2022;42:4117–33. <https://doi.org/10.3233/JIFS-212559>.
- Ramaraju SK, Kaliannan T, Ambrose Joseph S, Kumaravel U, Albert JR, Natarajan AV, et al. Design and experimental investigation on VL-MLI intended for half height (H-H) method to improve power quality using modified particle swarm optimization (MPSO) algorithm. *J Intell Fuzzy Syst* 2022;42:5939–56. <https://doi.org/10.3233/JIFS-212583>.
- Thangamuthu L, Albert JR, Chinnanan K, Gnanavel B. Design and development of extract maximum power from single-diode PV model for different environmental condition using BAT optimization algorithm. *J Intell Fuzzy Syst* 2022;43:1091–102. <https://doi.org/10.3233/JIFS-213241>.
- Gnanavel, C., Muruganantham, P., Vanchinathan, K., Johny Renoald, A.: Experimental Validation and Integration of Solar PV Fed Modular Multilevel Inverter (MMI) and Flywheel Storage System. 2021 IEEE Mysore Sub Section International Conference, MysuruCon 2021. 147–153 (2021). <https://doi.org/10.1109/MysuruCon52639.2021.9641650>.
- Albert JR, Selvan P, Sivakumar P, Rajalakshmi R. An advanced electrical vehicle charging station using adaptive hybrid particle swarm optimization intended for renewable energy system for simultaneous distributions. *J Intell Fuzzy Syst* 2022; 43:4395–407. <https://doi.org/10.3233/JIFS-220089>.
- Kaliannan T, Albert JR, Begam DM, Madhumathi P. Power Quality Improvement in Modular Multilevel Inverter Using for Different Multicarrier PWM. *European Journal of Electrical Engineering and Computer Science* 2021;5:19–27. <https://doi.org/10.24018/ejece.2021.5.2.315>.
- R.,r1., K.,S1, K.,P1, S.,A2, S.,C3, G.: An Experimental and Investigation on Asymmetric Modular Multilevel Inverter an Approach with Reduced Number of Semiconductor Devices. *J Electrical Systems* 2022;18:318–30. JOHNY,A1\*.,
- Atefat MA, Jahanbani Ardakani F. Maximum power point tracking of solar system using improved flower pollination algorithm. *Computational Intelligence in Electrical Engineering* 2021;12:49–60.
- Younis A, Bakhit A, Onsa M, Hashim M. A comprehensive and critical review of bio-inspired metaheuristic frameworks for extracting parameters of solar cell single and double diode models. *Energy Rep* 2022;8:7085–106. <https://doi.org/10.1016/j.egyr.2022.05.160>.
- M. Abbas, M., H. Muhsen, D.: Extraction of Double-Diode Photovoltaic Module Model'S Parameters Using Hybrid Optimization Algorithm. *Journal of Engineering and Sustainable Development*. 26, 77–91 (2022). <https://doi.org/10.31272/jeasd.26.4.9>.
- Moghassemi A, Ebrahimi S, Padmanaban S, Mitolo M, Holm-Nielsen JB. Two fast metaheuristic-based MPPT techniques for partially shaded photovoltaic system. *Int J Electr Power Energy Syst* 2022;137. <https://doi.org/10.1016/j.ijepes.2021.107567>.
- Bhos CD, Nasikkar PS. Optimization-based maximum power extraction from solar photovoltaic system under non-uniform irradiance. *Int J Ambient Energy* 2022;43: 6629–42. <https://doi.org/10.1080/01430750.2022.2037456>.
- Palanisamy R, Govindaraj V, Siddhan S, Albert JR. Experimental investigation and comparative harmonic optimization of AMLI incorporate modified genetic algorithm using for power quality improvement. *J Intell Fuzzy Syst* 2022;43: 1163–76. <https://doi.org/10.3233/JIFS-212668>.
- Dhanalakshmi B, Rajasekar N. Dominance square based array reconfiguration scheme for power loss reduction in solar PhotoVoltaic (PV) systems. *Energy Convers Manag* 2018;156:84–102. <https://doi.org/10.1016/j.enconman.2017.10.080>.
- Wang, M., Gao, B.: An Improved GWO Technique Integrated with P&O Algorithm for Photovoltaic System Considering Different Conditions in the Irradiance. *Proceedings of 2022 IEEE 5th International Electrical and Energy Conference, CIEEC 201013–1018* (2022). <https://doi.org/10.1109/CIEEC54735.2022.9846656>.
- Mishra, Vijay Laxmi, Yogesh K. Chauhan, and K. S. Verma. "A novel PV array reconfiguration approach to mitigate non-uniform irradiation effect." *Energy Conversion and Management* 265 (2022): 115728. 265, 115728 (2022).
- Manjunath, Suresh, H.N.R., Rajanna, S., Thanikanti, S.B., Alhelou, H.H.: Hybrid interconnection schemes for output power enhancement of solar photovoltaic array under partial shading conditions. *IET Renewable Power Generation*. 16, 2859–2880 (2022). <https://doi.org/10.1049/rpg.2.12543>.
- Johny renoald A: Solar Energy Assessment in Various Regions of Indian Sub-continent. (2020).
- Albert JR. Design and Investigation of Solar PV Fed Single-Source Voltage-Lift Multilevel Inverter Using Intelligent Controllers. *Journal of Control, Automation and Electrical Systems* 2022;33:1537–62. <https://doi.org/10.1007/s40313-021-00892-w>.
- Wang K, Du H, Jia R, Jia H. Performance Comparison of Bayesian Deep Learning Model and Traditional Bayesian Neural Network in Short-Term PV Interval Prediction. *Sustainability (Switzerland)* 2022;14. <https://doi.org/10.3390/su141912683>.
- Fan F, Na ZX, Zhang CZ, Li HR, Tong CL. Hot Spot Detection of Photovoltaic Module Infrared Near-field Image based on Convolutional Neural Network. *J Phys Conf Ser* 2022;2310. <https://doi.org/10.1088/1742-6596/2310/1/012076>.
- Wang K, Dowling AW. Bayesian optimization for chemical products and functional materials. *Curr Opin Chem Eng* 2022;36:1–22. <https://doi.org/10.1016/j.coche.2021.100728>.
- Periasamy, M., Kaliannan, T., Selvaraj, S., Manickam, V., Joseph, S.A., Albert, J.R.: Various PSO methods investigation in renewable and nonrenewable sources. 13, 2498–2505 (2022). <https://doi.org/10.11591/ijpeds.v13.i4.pp2498-2505>.
- Jayaudhaya J, Ramash Kumar K, Tamil Selvi V, Padmavathi N. Improved Performance Analysis of PV Array Model Using Flower Pollination Algorithm and

- Gray Wolf Optimization Algorithm. *Math Probl Eng* 2022;2022. <https://doi.org/10.1155/2022/5803771>.
- [32] Kaliannan T, Albert JR, Begam DM, Madhumathi P. Power Quality Improvement in Modular Multilevel Inverter Using for Different Multicarrier PWM 2021;5:19–27.
- [33] Dao TK, Nguyen TT, Nguyen VT, Nguyen TD. A Hybridized Flower Pollination Algorithm and Its Application on Microgrid Operations Planning. *Applied Sciences (Switzerland)* 2022;12. <https://doi.org/10.3390/app12136487>.
- [34] Rana AS, Nasir M, Khan HA. String level optimisation on grid-tied solar PV systems to reduce partial shading loss. *IET Renew Power Gener* 2018;12:143–8. <https://doi.org/10.1049/iet-rpg.2017.0229>.
- [35] Yousri D, Babu TS, Allam D, Ramchandaramurthy VK, Beshr E, Eteiba MB. Fractional chaos maps with flower pollination algorithm for partial shading mitigation of photovoltaic systems. *Energies (Basel)* 2019;12. <https://doi.org/10.3390/en12183548>.
- [36] Pei T, Hao X, Gu Q. A Novel Global Maximum Power Point Tracking Strategy Based on Modified Flower Pollination Algorithm for Photovoltaic Systems under Non-Uniform Irradiation and Temperature Conditions. *Energies (Basel)* 2018;11. <https://doi.org/10.3390/en11102708>.
- [37] Prasanth Ram J, Rajasekar N. A Novel Flower Pollination Based Global Maximum Power Point Method for Solar Maximum Power Point Tracking. *IEEE Trans Power Electron* 2017;32:8486–99. <https://doi.org/10.1109/TPEL.2016.2645449>.
- [38] Husain, M.A., Tariq, A., Hameed, S., Arif, M.S. bin, Jain, A.: Comparative assessment of maximum power point tracking procedures for photovoltaic systems. *Green Energy and Environment*. 2, 5–17 (2017). <https://doi.org/10.1016/j.gee.2016.11.001>.
- [39] Zaki Diab AA, Rezk H. Global MPPT based on flower pollination and differential evolution algorithms to mitigate partial shading in building integrated PV system. *Sol Energy* 2017;157:171–86. <https://doi.org/10.1016/j.solener.2017.08.024>.
- [40] Prasanth Ram J, Rajasekar N. A new global maximum power point tracking technique for solar photovoltaic (PV) system under partial shading conditions (PSC). *Energy* 2017;118:512–25. <https://doi.org/10.1016/j.energy.2016.10.084>.
- [41] Yang B, Zhu T, Wang J, Shu H, Yu T, Zhang X, et al. Comprehensive overview of maximum power point tracking algorithms of PV systems under partial shading condition. *J Clean Prod* 2020;268. <https://doi.org/10.1016/j.jclepro.2020.121983>.
- [42] Shankar N, SaravanaKumar N. Reduced Partial shading effect in Multiple PV Array configuration model using MPPT based Enhanced Particle Swarm Optimization Technique. *Microprocess Microsyst* 2020;103287. <https://doi.org/10.1016/j.micpro.2020.103287>.